# Evaluating the Communication Reliability of Earth–Moon Satellite Constellations Using Model Counting

Ioana-Roxana Băcălie

Delft University of Technology


TU Delft

# Evaluating the Communication Reliability of Earth–Moon Satellite Constellations Using Model Counting

by

Ioana-Roxana Băcălie

to obtain the degree of Master of Science
at the Delft University of Technology,
to be defended publicly on Tuesday June 23, 2026 at 13:00.

Thesis committee: Dr. Neil Yorke-Smith
Dr. Frans A. Oliehoek
Dr. Anna L.D. Latour
Dr. Max Bannach

Cover: Canadarm 2 Robotic Arm Grapples SpaceX Dragon by NASA under CC BY-NC 2.0 (Modified)
Style: TU Delft Report Style, with modifications by Daan Zwaneveld

An electronic version of this thesis is available at `http://repository.tudelft.nl/`.

TU Delft

# Acknowledgments

I would like to thank my supervisors, Dr. Anna L.D. Latour, Dr. Neil Yorke-Smith and Dr. Max Bannach for their support and guidance throughout the project. I am grateful for their feedback and the discussions that helped shape the direction of this thesis. This work has benefitted from Dr. Bannach's and Dr. Latour's participation in Dagstuhl Seminar 25362 "Optimization and Automated Reasoning for Designing Future Space Missions."

I would also like to thank my family and friends for their continued support, encouragement and patience throughout my studies and during the completion of this thesis.

*Ioana-Roxana Băcălie*
*Delft, June 2026*

# Summary

As interest in lunar missions continues to grow, reliable communication between the Earth and the Moon becomes increasingly important. One way to achieve such communication is through satellite constellations, in which satellites communicate through inter-satellite links. However, evaluating the reliability of such constellations is a challenging problem due to continuously changing satellite positions.

In this thesis, we study how the communication reliability of Earth–Moon satellite constellations can be modelled and evaluated. We represent the communication network as a probabilistic graph, in which vertices correspond to satellites and edges correspond to communication links. We consider two reliability metrics: the probability that communication exists between Earth and Moon ground-connected satellites and the probability that the entire network is connected. We also study hop-constrained variants of these metrics, as in quantum communication the number of relay hops is limited.

To evaluate the communication reliability of Earth-Moon satellite constellations, we use projected weighted model counting. Starting from Walker constellations around both the Earth and the Moon, we propagate satellite positions over time. At selected discrete timestamps, we build probabilistic networks to represent the constellation at that point in time. We then encode communication properties as propositional formulas and apply projected weighted model counting to compute reliability. We compare two encodings: one based on reachability, adapted from existing work, and one that explicitly models communication paths.

We evaluate the proposed approach on multiple constellation configurations and timestamps. The experiments provide insights into the factors affecting communication reliability and the computational performance of the two encodings. The results show that projected weighted model counting can be used to evaluate the reliability of dynamic Earth–Moon satellite communication networks, while also highlighting scalability challenges for larger problem instances.

# Contents

# 1 Introduction

## 1.1. Motivation

Interest in lunar exploration has increased significantly in recent years, as shown by initiatives such as ispace's HAKUTO-R missions [1] and NASA's Artemis programme [2]. Missions to the Moon require reliable communication with Earth to transmit scientific data and ensure mission safety and success. This communication can be achieved through satellite constellations, which already play an important role in modern infrastructure by supporting applications such as navigation, Earth observation, internet connectivity, and scientific missions. Plans for a lunar communication satellite constellation are already underway, as part of efforts to support a sustained human presence on the Moon [3].

The widespread use of satellite communication is reflected in the large number of satellites currently orbiting the Earth. There are over 12 000 such satellites, with the majority being used for communication purposes [4]. These satellites communicate either directly with ground stations or with each other through Inter-Satellite Links (ISLs). ISLs offer some advantages over communicating directly with ground stations, such as lower latency and greater efficiency [5]. However, the quality and availability of these links depend on many factors, such as communication range, weather conditions, hardware malfunctions, or positioning errors. As a result, communication paths between satellites and ground stations may not always be available. Establishing reliable communication requires maintaining a high probability that such paths exist. This highlights the importance of evaluating the reliability of satellite constellations, which is a challenging problem. Satellites continuously move along their orbits, and communication links appear and disappear over time, resulting in changes in the network topology.

Reliability evaluation becomes even more important when considering emerging communication technologies. Quantum communication, for example, imposes constraints on the number of relay hops. It is an emerging communication technology that significantly improves communication security by leveraging the principles of quantum mechanics [6]. However, quantum states are highly prone to decoherence and transmission loss [7]. Thus, each additional communication hop increases the risk of degrading the transmitted quantum information, making the path length an important consideration in satellite communication networks. These challenges motivate the need for methods that can evaluate the reliability of Earth–Moon satellite communication networks.

## 1.2. Research Objective

Previous work has shown that projected weighted model counting can be used to estimate the reliability of satellite constellations with inter-satellite links [8]. However, this work focuses on communication networks around a single celestial body and does not consider communication networks spanning both the Earth and the Moon. Extending reliability analysis to such networks is necessary for evaluating future Earth–Moon communication infrastructures. For this reason, in this thesis, we extend the work on satellite constellation reliability estimation to communication networks spanning two celestial bodies.

The objective of this thesis is to model and evaluate the communication reliability of Earth–Moon satellite

constellations. To achieve this, we represent Earth–Moon communication networks as probabilistic graphs and evaluate communication reliability using projected weighted model counting.

## 1.3. Contributions

The main contributions of this thesis are:

- An extension of probabilistic satellite constellation reliability analysis from communication networks around a single celestial body to communication networks spanning both the Earth and the Moon, presented in Chapter 4.
- The application of an encoding for formulas based on reachability, adapted from existing work, and one that explicitly models communication paths to Earth–Moon satellite constellation reliability analysis.
- An experimental analysis on how hop constraints and constellation setup influence communication reliability and computational performance over time, presented in Chapter 6.

## 1.4. Thesis Outline

The remainder of this thesis is structured as follows:

**Chapter 2 – Background** introduces the theoretical foundations required for this thesis. We cover satellite constellations, graphs, propositional logic, and projected weighted model counting.

**Chapter 3 – Related Work** summarises related work on network reliability and weighted model counting, and identifies the research gap this thesis addresses.

**Chapter 4 – Problem Definition** formalises the Earth–Moon communication reliability problem. It introduces the Earth–Moon network model, describes the computation of communication link probabilities, and defines the reliability metrics considered in this thesis.

**Chapter 5 – Approach** presents the proposed framework. It explains how the Earth–Moon satellite constellations are generated, how probabilistic communication graphs are constructed, the two propositional encodings used in this work, and how projected weighted model counting is applied to compute reliability.

**Chapter 6 – Experiments & Results** presents the experimental setup and the results. The experiments focus on evaluating the impact of hop constraints and constellation configurations on communication reliability and computational performance over time.

**Chapter 7 – Conclusion & Future Work** summarises the main findings of this thesis, discusses its limitations, and outlines directions for future research.

# 2 Background

In this chapter, we introduce the concepts that form the basis of the modelling and reliability evaluation approach developed in this thesis. We first present the astrodynamics concepts used to generate Earth–Moon satellite constellations. We then introduce theoretical concepts about graphs used to model communication networks, followed by propositional logic and weighted model counting.

## 2.1. Space Systems

In this section, we briefly introduce the astrodynamics concepts required to understand this thesis. For a more comprehensive overview of orbital mechanics and satellite systems, we refer the reader to textbooks such as *Fundamentals of Astrodynamics* [9] and *Space Mission Analysis and Design* [10].

### 2.1.1. Satellite constellations

Satellites are objects that orbit around another body and can be either natural, like the Moon, or artificial. Artificial satellites have a variety of uses, including communication relay, weather forecasting, navigation, broadcasting, scientific research, and Earth observation.

A satellite constellation is a coordinated system of multiple artificial satellites that work together for the same purpose. Satellites are positioned to provide continuous coverage over regions of one or more celestial bodies and communicate with ground stations. Satellites in such constellations communicate through inter-satellite links.

One common arrangement for satellites is the Walker Delta constellation [11], in which satellites are evenly distributed across several orbital planes. The notation for Walker constellations is $i : t/p/f$, where:

- $i$ is the orbital inclination;
- $t$ is the total number of satellites;
- $p$ is the number of equally spaced orbital planes;
- $f$ is the relative spacing between satellites in adjacent planes.

### 2.1.2. Astronomical and Orbital Mechanics

In celestial mechanics, a Kepler orbit describes the motion of one body relative to another, which forms a two-dimensional orbital plane in three-dimensional space. The Keplerian model considers only the gravitational attraction of two bodies and neglects other factors that influence the system, such as perturbations due to gravitational interactions with other objects, atmospheric drag, solar radiation pressure, and a non-spherical central body.

Keplerian orbits can be fully described by six orbital elements, named Keplerian elements, which can be visualised in figure 2.1. Three of these elements define the orientation of the orbital plane:

- Inclination ($i$): the angle between the orbital plane and the reference plane, typically chosen as the equatorial plane of the central body. The angle is measured at the ascending node (where the orbit crosses the reference plane). Values near 0° correspond to equatorial orbits, and values near 90° correspond to polar orbits.
- Longitude of the ascending node ($\Omega$): the angle from the ascending node of the orbit to the reference direction of the reference frame, measured in the reference plane. It is also known as the right ascension of the ascending node.
- Argument of periapsis ($\omega$): the orientation in the orbital plane, as an angle measured from the ascending node to the periapsis (the closest point to which the satellite body reaches the primary body around which it orbits).

Two Keplerian elements define the size and shape of the trajectory:

- Semi-major axis (a): half the distance between the apoapsis and periapsis, where the periapsis is the point closest to the primary body and the apoapsis is the point farthest from it.
- Eccentricity (e): shape of the ellipse, describing how much it deviates from a perfect circle. An eccentricity of zero describes a perfect circle, values less than 1 describe an ellipse, values greater than 1 describe a hyperbolic trajectory, and a value of exactly 1 describes a parabola.

The last Keplerian element is true anomaly ($\nu$), which defines the position of the orbiting body along the trajectory, measured from periapsis.

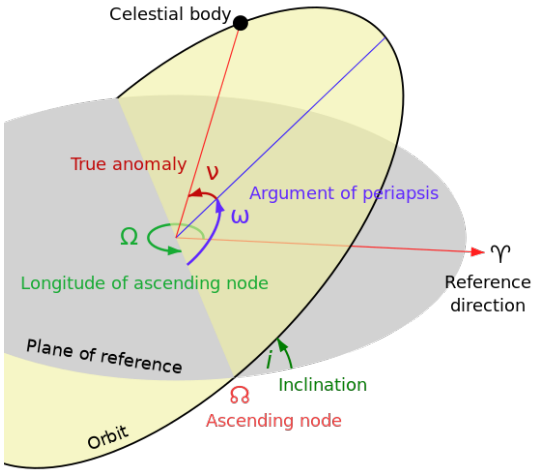


**Figure 2.1:** Keplerian orbital elements. Source: Lasunncty (Wikipedia), CC BY-SA 3.0 [12].

The orbital motion of satellites is commonly described using the six classical Keplerian elements introduced above. However, Keplerian elements become singular for circular and equatorial orbits. For this reason, some astrodynamics libraries, including PyKep, use equinoctial elements as an alternative orbital representation. Equinoctial elements are denoted by $p$, $f$, $g$, $h$, $k$, and $L$, and are defined in terms of the classical Keplerian elements as follows:

$$p = a\,(1 - e^2), \tag{2.1}$$
$$f = e\,\cos(\omega + \Omega), \tag{2.2}$$
$$g = e\,\sin(\omega + \Omega), \tag{2.3}$$
$$h = \tan\left(\frac{i}{2}\right)\cos\Omega, \tag{2.4}$$
$$k = \tan\left(\frac{i}{2}\right)\sin\Omega, \tag{2.5}$$
$$L = \Omega + \omega + \nu, \tag{2.6}$$

where:

- $a$ is the semi-major axis,
- $e$ is the eccentricity,
- $i$ is the inclination,
- $\Omega$ is the longitude of the ascending node,
- $\omega$ is the argument of periapsis,
- $\nu$ is the true anomaly.

The orbital state vectors of an orbit are Cartesian vectors of position ($r$) and velocity ($v$), which together with their time uniquely determine the trajectory of the orbiting body in space. In Chapter 4, we describe how satellite positions computed from these orbital elements are used to construct Earth–Moon communication networks at discrete timestamps.

## 2.2. Graphs

A graph is defined as a pair $G = (V, E)$, where $V$ is a set of vertices (nodes) and $E$ is a set of edges connecting pairs of vertices. Graphs may be directed or undirected. In a directed graph (or digraph), each edge is an ordered pair $(u, v) \in E$, representing a connection from vertex $u$ to vertex $v$. In an undirected graph, edges are unordered pairs $(u, v)$, representing bidirectional connections between vertices. A weighted graph is a graph in which a numerical weight $w : E \to \mathbb{R}$ is assigned to each edge.

A path in a graph $G = (V, E)$ is a sequence of vertices

$$(v_0, v_1, \ldots, v_k)$$

such that $\{v_i, v_{i+1}\} \in E$ for every $i \in \{0, \ldots, k-1\}$, and $v_i \neq v_j$ whenever $i \neq j$. The length of the path is the number of edges that it contains. A graph is connected if there exists a path between every pair of vertices in the graph.

In this thesis, we model Earth–Moon satellite constellations as probabilistic undirected graphs. Satellites correspond to vertices and communication links correspond to edges. Reliability properties can therefore be expressed as graph properties. In Chapter 4, we describe in detail how Earth–Moon constellations are modelled as such graphs.

## 2.3. SAT and model counting foundations

We briefly recall some concepts of propositional logic, SAT solving, and model counting from the literature that form the basis of the reliability encodings used throughout this thesis. For a more detailed overview, we refer the reader to textbooks, for example *Mathematical Logic for Computer Science* [13] or *Handbook of satisfiability* [14].

### 2.3.1. Propositional logic

A propositional formula $\varphi$ is defined over a finite set of Boolean variables $\mathcal{X} = \{X_1, X_2, \ldots, X_n\}$, which are combined using logical connectives such as disjunction $\vee$ (*or*), conjunction $\wedge$ (*and*), and negation $\neg$ (*not*). A *literal* is either a propositional variable $X \in \mathcal{X}$ or its negation $\neg X$. A *clause* is a disjunction of literals. Propositional formulas are constructed inductively from literals using the available logical connectives.

A truth assignment $\tau : \mathcal{X} \to \{\top, \bot\}$ assigns a truth value to every variable in $\mathcal{X}$. A formula $\varphi$ is satisfied by $\tau$ if it evaluates to true under $\tau$, and $\varphi$ is satisfiable if there exists at least one assignment that satisfies it.

A formula is in **conjunctive normal form** (CNF) if it is a conjunction of clauses, i.e.

$$\varphi = C_1 \wedge C_2 \wedge \cdots \wedge C_n,$$

where each $C_i$ is a clause.

A formula is in **disjunctive normal form** (DNF) if it is a disjunction of conjunctions, i.e.

$$\varphi = C_1 \vee C_2 \vee \cdots \vee C_n,$$

where each $C_i$ is a term.

### 2.3.2. SAT and CNF encoding

The Boolean satisfiability problem (SAT) asks, given a propositional formula $\varphi$, whether there exists a truth assignment $\tau$ that satisfies it. SAT is proven to be NP-complete [15]. Despite this, modern SAT solvers are highly efficient in practice and can handle formulas with millions of variables and clauses. Most SAT solvers expect their input in CNF, which is why converting propositional formulas into CNF is an important preprocessing step.

A naive approach for transforming a propositional formula into CNF is to repeatedly apply Boolean algebra rules. However, this approach can lead to an exponential increase in the size of the resulting formula. A more efficient method is **Tseitin encoding** [16], which converts any propositional formula into an equisatisfiable CNF formula of linear size. This transformation introduces auxiliary variables that represent subformulas of the original formula, along with additional clauses that encode the equivalence between the auxiliary variables and their corresponding subformulas.

As an example, consider the following DNF formula:

$$(a \wedge b) \vee (d \wedge \neg e) \vee (\neg b \wedge \neg c).$$

Tseitin encoding introduces the following auxiliary variables:

$$v_1 \leftrightarrow (a \wedge b)$$

$$v_2 \leftrightarrow (d \wedge \neg e)$$

$$v_3 \leftrightarrow (\neg b \wedge \neg c)$$

so that the original formula is rewritten as $v_1 \vee v_2 \vee v_3$. Each equivalence is then converted into CNF clauses. For example:

$$\begin{aligned} &v_1 \leftrightarrow (a \wedge b) \\ &\quad \equiv (\neg v_1 \vee a) \wedge (\neg v_1 \vee b) \wedge (v_1 \vee \neg a \vee \neg b) \end{aligned}$$

The remaining equivalences are encoded similarly, and the final CNF formula is the conjunction of all such clauses together with the clause $(v_1 \vee v_2 \vee v_3)$.

CNF formulas are commonly represented using the DIMACS file format, a plain-text format originally introduced as part of the DIMACS Challenge [17]. DIMACS is the standard input format for most SAT and model counting tools. These encodings form the input format for the projected weighted model counting solver used in this thesis.

### 2.3.3. Weighted Model Counting

Model counting, also known as #SAT, is the problem of computing the number of distinct satisfying truth assignments for a propositional formula. Such assignments are called models of that given formula. The model counting problem is known to be a #P-complete problem. Let $\mathcal{M}(\varphi)$ denote the set of all satisfying assignments (models) of a propositional formula $\varphi$. The model count of $\varphi$ is then defined as

$$\#(\varphi) = |\mathcal{M}(\varphi)|.$$

Weighted model counting extends this by associating a weight $w(\ell)$ with each literal $\ell$. The weight of a model $\tau \in \mathcal{M}(\varphi)$ is the product of the weights of the literals:

$$w(\tau) = \prod_{X \in \mathcal{X}} w(\ell_X^\tau),$$

where $\ell_X^\tau = X$ if $\tau(X) = \top$, and $\ell_X^\tau = \neg X$ if $\tau(X) = \bot$. The weighted model count is then defined as

$$WMC(\varphi) = \sum_{\tau \in \mathcal{M}(\varphi)} w(\tau).$$

Projected model counting restricts counting to a subset of variables $\mathcal{P} \subseteq \mathcal{X}$, called projection variables or show variables. Two models that agree on all variables in $\mathcal{P}$ but differ on variables in $\mathcal{X} \setminus \mathcal{P}$ are treated as equivalent, and counted only once. Let $\tau|_\mathcal{P}$ denote the restriction of a model $\tau$ to $\mathcal{P}$, and let

$$\mathcal{M}_\mathcal{P}(\varphi) = \{\tau|_\mathcal{P} \mid \tau \in \mathcal{M}(\varphi)\}$$

denote the set of projected models. Projected weighted model counting (PWMC) then computes

$$PWMC_\mathcal{P}(\varphi) = \sum_{\sigma \in \mathcal{M}_\mathcal{P}(\varphi)} \sum_{\substack{\tau \in \mathcal{M}(\varphi) \\ \tau|_\mathcal{P} = \sigma}} w(\tau).$$

In this thesis, we reduce reliability evaluation to a projected weighted model counting problem. After modelling Earth–Moon communication networks as probabilistic graphs, we encode communication properties as propositional formulae. To obtain these formulae, we introduce auxiliary variables that should not affect the computed probability, which is why projection is necessary. In Chapter 5, we describe in detail how these formulae are constructed and how PWMC is used to compute connectivity probabilities.

# 3

# Related Work

In this chapter, we discuss previous work relevant to this thesis. We first discuss previous work on reliability and connectivity analysis in communication and satellite networks. We then discuss advances in model counting and weighted model counting that form the computational basis of our approach. We also identify the research gap that this thesis addresses and explain how our work builds on and extends existing research.

## 3.1. Network Reliability

Network reliability has been studied across many domains, including power grids, transportation systems, and communication infrastructure. In communication networks, it typically refers to the probability that communication can be established between nodes when links fail with some probability. The problem of computing exact network reliability is computationally difficult. It is known to be #P-complete [18, 19]. Unless P = NP, no polynomial-time algorithm exists for solving #P-complete problems, and exact computation therefore becomes infeasible as the size of the network grows. Despite this, exact reliability analysis remains important for obtaining reliable ground truths and for evaluating the quality of approximations [8].

Several studies have investigated the reliability of satellite constellations and inter-satellite communication networks. Leyva et al. [20] and Lee et al. [21] study connectivity and reliability properties of low Earth orbit (LEO) satellite constellations, while Radhika et al. [22] and Ruibo et al. [23] consider fault tolerance and survivability under link failures. Duenas et al. [24] analyse reliability in the context of satellite communication routing.

Other work has approached exact reliability analysis using Binary Decision Diagrams (BDDs) [25, 26, 27], exploiting the compact symbolic representation that BDDs provide for Boolean functions. More recently, model counting and weighted model counting techniques have been applied to reliability analysis [28, 29, 30], offering a flexible framework for encoding and solving complex reliability queries. Many of these methods rely on heuristic or approximation-based techniques for estimating connectivity and reliability properties. However, as highlighted in [8], such approaches do not provide exact reliability values.

The main inspiration for this thesis is the work of Bannach et al. [8], who introduce reliability metrics for satellite constellations with inter-satellite communication and show how these metrics can be computed by encoding connectivity properties into propositional logic and solving them using weighted model counting. They study metrics such as pairwise connectivity probability and overall network connectivity probability. To compute these metrics, they introduce an encoding that uses auxiliary variables to represent whether a node is reachable from a source node. In this work, we adopt this encoding and apply it to Earth–Moon satellite constellations. Furthermore, they model satellite communication networks as dynamic graph snapshots evaluated over discrete timestamps.

A similar snapshot-based view of satellite networks is also used by Xu et al. [31], who study the

robustness of satellite constellation networks under different attack strategies and routing mechanisms. In their work, the continuously changing satellite topology is discretised into a sequence of graph snapshots over time. This is closely related to the modelling approach used in this thesis, where Earth–Moon communication networks are represented as dynamic probabilistic graphs evaluated at discrete timestamps.

However, the experiments in [8] are limited to relatively small satellite constellations around a single celestial body. In this thesis, we extend their modelling approach and logical encodings to long-distance communication networks that span both the Earth and the Moon. This introduces additional challenges, including different satellite communication roles and the dynamic relative motion between Earth and the Moon that continuously reshapes the network topology.

## 3.2. Probabilistic Reasoning and Weighted Model Counting

The applicability of model counting spans a wide range of domains, including probabilistic reliability analysis and combinatorial optimisation. Since 2020, yearly model counting competitions have been organised to evaluate modern counting approaches and solvers [32]. These competitions resulted in significant progress in the efficiency and scalability of exact counting tools, with submissions covering a wide range of algorithmic approaches.

Recent work has explored techniques such as projected model counting [33], structure-guided reasoning [34], and algebraic decision diagrams for weighted model counting [35]. Together, these developments have significantly improved the scalability of exact counting techniques and enabled reliability analysis for increasingly large probabilistic systems. In this thesis, we perform projected weighted model counting using the Ganak solver [36, 37], a state-of-the-art model counting tool that supports weighted and projected counting.

## 3.3. Research gap

Previous work has extensively studied network reliability, satellite communication networks, and probabilistic reasoning techniques such as weighted model counting. However, existing approaches mainly focus on satellite constellations orbiting a single celestial body. To the best of our knowledge, reliability analysis for dynamic probabilistic communication constellations spanning both the Earth and the Moon has not yet been studied. Extending reliability analysis to Earth–Moon networks is not straightforward. The two constellations orbit different celestial bodies, satellites take on different communication roles, and the relative motion between Earth and the Moon continuously changes the network topology, making the problem more complex than single-body constellations.

In this thesis, we address this gap by extending the approach of Bannach et al. [8] to satellite constellations orbiting two different celestial bodies. We model Earth–Moon satellite communication networks as dynamic probabilistic graphs and analyse their reliability using projected weighted model counting.

# 4

# Problem definition

In this chapter, we formalise the Earth-Moon satellite communication model addressed in this thesis. We first describe how we represent satellite constellations as time-dependent communication networks and introduce the different types of satellites. Next, we define how we compute communication link probabilities from the geometric properties of the constellation. We also introduce the reliability measures used throughout this thesis.

## 4.1. Earth-Moon network model

We model satellites in a constellation as nodes in a weighted network, where edges represent direct communication links between satellites. We assign each edge a weight that corresponds to the probability that the two satellites can communicate successfully. To avoid including communication links with negligible probabilities, we only consider edges whose communication probability exceeds 0.05. A weight of 1 means that the corresponding link between the satellites is fully reliable, which means that communication between the two satellites is always possible.

We assess the reliability of a satellite constellation by studying how the communication network evolves over time. We represent the communication network as a sequence of undirected probabilistic graphs.

$$G_t = (V_t, E_t),$$

where $t \in T$ denotes a discrete timestamp. The set $V_t$ represents the satellites at timestamp $t$, while $E_t$ represents the set of edges between satellites at that timestamp.

We distinguish three different types of satellite communication capabilities:

- communication with ground stations,
- communication with satellites orbiting the opposite celestial body (Earth–Moon),
- communication with close-by satellites, orbiting the same celestial body.

Based on these communication capabilities, we divide the satellites into the following categories, which are illustrated in Figure 4.1:

- $L_M$ and $L_E$ denote the satellites that are capable of long-range communication between the Earth and the Moon. $L_M$ represents the group of satellites that orbit the Moon, while $L_E$ represents the group of satellites that orbit the Earth. These satellites can also communicate with nearby satellites orbiting the same celestial body.
- $GS_M$ and $GS_E$ are the satellites that can communicate with ground stations, orbiting the Moon and the Earth, respectively. We assume that these satellites maintain communication with ground stations at all times, independently of their position in space. Therefore, the exact locations of ground stations are not taken into consideration in our model.

- $S_M$ and $S_E$ are the groups of short-range satellites that are neither capable of communicating over long-range distances, nor with ground stations. These satellites can only communicate with nearby satellites orbiting the same celestial body.

Therefore,

$$V_t = L_{M,t} \cup L_{E,t} \cup GS_{M,t} \cup GS_{E,t} \cup S_{M,t} \cup S_{E,t}.$$

To simplify the communication model, we make the following assumptions:

- We consider the Earth fixed in an Earth-centred reference frame.
- Communication probabilities depend only on inter-satellite distance.
- Ground-connected satellites maintain communication with ground stations at all times.

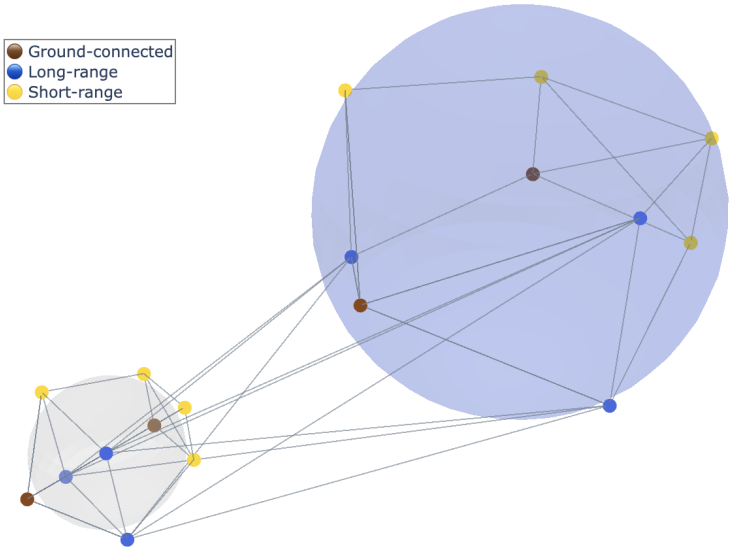


**Figure 4.1:** Example Earth–Moon communication network

## 4.2. Edge probabilities computation

To evaluate network reliability, we associate each communication link in the graph with a probability of successful communication. Many factors can influence the probability that two satellites communicate with each other: weather conditions, geographic obstacles, distance, positioning errors, hardware failures, or signal interference. However, the purpose of this work is to study the reliability framework rather than a specific communication technology. Therefore, we model link probabilities as a function of inter-satellite distance.

Let $\mathbf{r}_1 = (x_1, y_1, z_1)$ and $\mathbf{r}_2 = (x_2, y_2, z_2)$ be the Cartesian position vectors of two satellites. We define the Euclidean distance between the satellites as the norm of the vector pointing from $\mathbf{r}_1$ to $\mathbf{r}_2$:

$$d(\mathbf{r}_1, \mathbf{r}_2) = \|\mathbf{r}_2 - \mathbf{r}_1\| = \sqrt{(x_2 - x_1)^2 + (y_2 - y_1)^2 + (z_2 - z_1)^2}.$$

Inter-satellite distances vary significantly depending on the constellation geometry. For instance, in the Galileo constellation, the maximum inter-satellite distance is approximately 59 000 km, corresponding to the orbital diameter, while the mean distance is approximately 42 000 km [38]. In the case of a satellite constellation that ensures communication between the Moon and Earth, distances increase substantially: the distance between Moon and Earth is approximately 384 400 km, and only a subset of satellites are capable of supporting communication over such ranges.

We calculate the communication probability of a link based on the inter-satellite distance. The probability of successful communication decreases as the distance increases. Beyond a maximum

distance, communication is assumed to be impossible. We distinguish between communication links connecting satellites orbiting the same celestial body and long-range communication links connecting satellites orbiting different celestial bodies. We first define this probability model for satellites orbiting the same celestial body.

We introduce distance thresholds for both the Moon and the Earth: $d_{\text{rel}}$, representing the maximum distance at which communication between satellites is fully reliable, and $d_{max_M}$ and $d_{max_E}$, representing the distances beyond which communication is no longer possible on the Moon and the Earth, respectively, with

$$d_{\text{rel}} < d_{max_M}, \quad d_{\text{rel}} < d_{max_E}.$$

We define $d_{\text{rel}}$ as a fixed value for both the Earth and the Moon. To model the likelihood of communication between satellites based on their relative distances, we define a function that converts Euclidean distances into probabilities. Specifically, given $d_{ij}$ as the distance between satellites $i$ and $j$, we compute the communication probability $p_{ij}$ as follows:

For satellites orbiting the Moon:

$$p_{ij_M} = \begin{cases} 1 & \text{if } d_{ij} \leq d_{\text{rel}}, \\ \dfrac{d_{max_M} - d_{ij}}{d_{max_M} - d_{\text{rel}}} & \text{if } d_{\text{rel}} < d_{ij} < d_{max_M}, \\ 0 & \text{if } d_{ij} \geq d_{max_M}. \end{cases} \tag{4.1}$$

For satellites orbiting the Earth:

$$p_{ij_E} = \begin{cases} 1 & \text{if } d_{ij} \leq d_{\text{rel}}, \\ \dfrac{d_{max_E} - d_{ij}}{d_{max_E} - d_{\text{rel}}} & \text{if } d_{\text{rel}} < d_{ij} < d_{max_E}, \\ 0 & \text{if } d_{ij} \geq d_{max_E}. \end{cases} \tag{4.2}$$

This ensures that:

- Probabilities are always in the range $[0, 1]$.
- Satellites that are closer together have a higher probability of communication.
- Satellites that are very far apart have a probability approaching zero.

To determine the values of $d_{\text{max}_M}$ and $d_{\text{max}_E}$, we rely on geometry. Let $h_M$ and $h_E$ denote the altitude of the satellites above the surface of the Moon and the Earth, respectively, and let $R_M$ denote the radius of the Moon and $R_E$ the radius of the Earth. The orbital radius for satellites orbiting the Moon is then given by $r_{\text{sat}_\text{M}} = R_M + h_M$ and for the Earth by $r_{\text{sat}_\text{E}} = R_E + h_E$

Assuming two satellites are at the same orbital altitude, we determine the maximum communication distance using the line-of-sight constraint. In the limiting case, the line connecting the two satellites is tangent to the surface. This yields:

$$d_{\text{max}_M} = \sqrt{2}\, r_{\text{sat}_\text{M}} = \sqrt{2(R_M + h_M)^2} \tag{4.3}$$

$$d_{\text{max}_E} = \sqrt{2}\, r_{\text{sat}_\text{E}} = \sqrt{2(R_E + h_E)^2} \tag{4.4}$$

For satellites orbiting different celestial bodies, communication is only possible between satellites that are capable of long-range communication. Communication also requires an unobstructed line of sight between the satellites. For each pair of Earth and Moon satellites, we first determine whether the straight line segment connecting them intersects either the Earth or the Moon. If such an intersection exists, communication is assumed to be impossible and no communication link is created. We compute the

communication probability based on their inter-satellite distance only for satellite pairs with a clear line of sight.

We introduce two distance thresholds for long-range communication:

- $d_{\text{rel}_{\text{LR}}}$: distance below which communication is considered reliable,
- $d_{\text{max}_{\text{LR}}}$: maximum distance at which communication is still possible.

Let $d_{EM}$ denote the Earth–Moon distance at a given timestamp, and let $a_E$ and $a_M$ denote the orbital radii of the Earth and Moon satellites, respectively. The thresholds are determined geometrically:

$$d_{rel_{LR}} = d_{EM} - a_E - a_M, \tag{4.5}$$

$$d_{max_{LR}} = d_{EM} + a_E + a_M. \tag{4.6}$$

The first threshold corresponds approximately to satellites positioned on the sides of their respective celestial bodies facing each other, while the second corresponds to satellites located on opposite sides. Let $d_{ij}$ denote the distance between a satellite $i$ orbiting the Moon and a satellite $j$ orbiting the Earth. The communication probability is then defined as follows:

$$p_{ij_{LR}} = \begin{cases} 1 & \text{if } d_{ij} \leq d_{\text{rel}_{\text{LR}}}, \\ \dfrac{d_{max_{LR}} - d_{ij}}{d_{max_{LR}} - d_{\text{rel}_{\text{LR}}}} & \text{if } d_{\text{rel}_{\text{LR}}} < d_{ij} < d_{max_{LR}}, \\ 0 & \text{if } d_{ij} \geq d_{max_{LR}}. \end{cases} \tag{4.7}$$

## 4.3. Reliability metrics

We express network reliability as the probability that certain connectivity properties hold in a probabilistic graph. Bannach et al. identify three probabilities that are relevant for assessing the reliability of a communication network [8]:

- probability that an $s$–$t$ path exists,
- probability that the network is connected,
- probability that a short $s$–$t$ path exists

In this thesis, we study two main reliability metrics. The first is the probability that communication exists between a ground-connected satellite orbiting the Earth and a ground-connected satellite orbiting the Moon. We are therefore interested in the probability that communication exists between nodes $s \in GS_E$ and $t \in GS_M$. This measure captures whether communication between the Earth and the Moon is possible at a given timestamp. The second metric we consider is the probability that the entire communication network is connected.

For each reliability measure, we distinguish between:

- unrestricted communication paths,
- short communication paths containing at most $k$ hops.

As discussed in Chapter 1, hop-constrained communication is relevant for quantum communication systems, where the number of intermediate relay satellites may affect communication quality. We therefore consider four reliability measures in this thesis:

- Earth–Moon communication reliability,
- hop-constrained Earth–Moon communication reliability,
- network connectivity reliability,
- hop-constrained network connectivity reliability.

# 5

# Approach

This chapter presents the approach and implementation used to analyse the reliability of Earth-Moon satellite communication networks. Building on the work from Bannach et al. [8], we model satellite constellations as probabilistic communication graphs and evaluate reliability using Projected Weighted Model Counting.

The proposed framework consists of the following steps:

1. generation of dynamic Earth–Moon satellite constellations and propagation through time
2. construction of probabilistic communication graphs at different timestamps
3. encoding of reliability metrics into propositional logic for each constructed probabilistic graph
4. exact reliability computation using PWMC

Instead of considering a single static graph, the system is represented as a sequence of graphs generated at different timestamps. For each timestamp, the following steps are performed:

1. propagate the positions of the satellites and the Moon,
2. compute pairwise inter-satellite distances,
3. compute communication probabilities,
4. construct the corresponding communication graph,
5. perform reliability calculations on the resulting graph.

## 5.1. Earth-Moon Constellation Generation

We model the Earth-Moon constellation as a time-dependent graph. We assume the Earth to be fixed, while the Moon is propagated around the Earth and the satellites are propagated around their respective central bodies. The communication graph evolves over time due to both satellite motion and the relative motion of the Moon around the Earth.

We model the Earth and Moon satellite constellation as two Walker Delta constellations introduced in Chapter 2: one constellation orbiting Earth and one constellation orbiting the Moon. The Moon is also propagated around Earth using orbital elements. For each constellation, we configure several parameters:

- orbital inclination
- orbital altitude
- total number of satellites
- number of orbital planes
- phasing factor

- number of ground-connected satellites
- number of long-range satellites

The ground-connected and long-range satellites are distributed uniformly across the constellation. This avoids clustering specific communication roles within the same region. These two categories are assigned disjointly, meaning a satellite cannot simultaneously belong to both groups.

We propagate satellite and Moon positions over time using Keplerian orbital mechanics. At each timestamp, the Cartesian coordinates of all satellites are extracted and used to compute pairwise inter-satellite distances, which form the basis for the communication probability model described in Section 4.2.

## 5.2. Encodings

The reliability metrics defined in Chapter 4 must be translated into propositional formulas before they can be computed. Different propositional encodings can vary in size, which affects the efficiency of the reliability computation. We consider two different encodings and we later compare them in terms of CNF size and runtime performance.

### 5.2.1. Reachability-based encoding

Bannach et al. [8] propose a reachability-based propositional encoding for computing network reliability. For a source $s$ and target $t$, they introduce auxiliary variables $r_v$ for each vertex, representing whether the node is reachable from $s$. The formula

$$\varphi_{st} = (r_s) \wedge (\neg r_t) \wedge \bigwedge_{u \in V(G)} \bigwedge_{\{u,v\} \in E(G)} (r_u \wedge e_{uv} \rightarrow r_v) \tag{5.1}$$

computes the probability that no $s$–$t$ path exists. The formula enforces that the source node $s$ is reachable, while the target node $t$ is not reachable. Furthermore, if a node $u$ is reachable and the edge $u, v$ exists, then node $v$ must also be reachable. The probability that a path exists can then be obtained by taking the complement.

They extend this idea to global connectivity and hop-constrained reachability using layered graph expansions. We adopt these encodings and apply them to the communication graphs obtained in the Earth-Moon setting. For a complete description of the construction and correctness proofs, we refer the reader to Bannach et al., *Reliability of Constellations with Inter-Satellite Communication* [8].

Based on these encodings, we can derive the number of variables and clauses required by the resulting CNF formulas. These quantities provide an indication of the size of the generated formulas and help explain the computational behaviour observed in the experiments. In Chapter 6, we compare the encodings in terms of the number of variables, number of clauses, and computation time, allowing us to investigate how the size of an encoding influences its computational performance.

Let ($|V|$) be the number of vertices and ($|E|$) the number of undirected edges. For the basic probability of a path encoding, the number of variables is $|E| + |V|$. The encoding contains $2|E|$ implication clauses, together with the two unit clauses $r_s$ and $\neg r_t$. Hence, the number of clauses is $2|E| + 2$. For the connected-network variant, the reachability encoding is applied to every unordered pair of vertices. This gives $|E| + \binom{|V|}{2}|V|$ variables and $\binom{|V|}{2}(2|E| + 2)$ clauses. For the hop-constrained probability of a path, reachability variables are introduced for each vertex and each layer (0,. . . ,k). The number of variables is $|E| + (k + 1)|V|$. The number of clauses is $2k|E| + 2$.

### 5.2.2. Path-based encoding

The reachability-based encoding is compact for the basic probability of a path between two nodes case, but grows significantly when extended to global connectivity or hop-constrained reachability. Computing connectivity requires multiple copies of the graph, while hop-constrained reliability requires a full layered expansion, both of which introduce more variables and clauses.

A natural question is therefore whether a simpler alternative encoding exists. We consider an alternative encoding, in which the reliability formula is constructed directly from the paths in the graph. While this approach also introduces auxiliary variables since we use Tseitin encoding, its structure is uniform across all probabilities. Comparing the two approaches allows us to assess whether the structural complexity introduced by the reachability encoding provides a practical computational advantage, or whether the simpler path-based formulation is competitive in the settings we consider.

Let $P_{st}$ denote the set of all simple paths between $s$ and $t$. For a path

$$p = (v_0, v_1, \ldots, v_k),$$

the path exists if all edges on the path exist simultaneously. This can be expressed as

$$\bigwedge_{i=0}^{k-1} e_{v_i v_{i+1}}.$$

The existence of at least one valid $s$-$t$ path is therefore represented by the formula

$$\varphi_{st} = \bigvee_{p \in P_{st}} \left( \bigwedge_{\{u,v\} \in p} e_{uv} \right). \tag{5.2}$$

This formula has DNF structure, but a direct conversion to CNF is computationally expensive due to the combinatorial blow-up caused by transforming large disjunctions of conjunctions. While this works for very small graphs, such as the graph from Example 1 with 10 nodes, it does not scale to larger instances.

To address this issue, we instead use a Tseitin-style encoding in which auxiliary variables are introduced to represent complete paths. For every path $p$ containing more than one edge, we introduce one auxiliary variable $x_p$ defined by the equivalence:

$$x_p \leftrightarrow \bigwedge_{\{u,v\} \in p} e_{uv}.$$

The equivalence is encoded in CNF using the implications

$$x_p \rightarrow e_{uv} \qquad \text{for every edge } \{u, v\} \in p, \tag{5.3}$$

and

$$\left( \bigwedge_{\{u,v\} \in p} e_{uv} \right) \rightarrow x_p. \tag{5.4}$$

In CNF form, this produces the clauses

$$(\neg x_p \vee e_1), (\neg x_p \vee e_2), \ldots, (\neg x_p \vee e_n),$$

together with the clause

$$(x_p \vee \neg e_1 \vee \neg e_2 \vee \cdots \vee \neg e_n),$$

where $e_1, \ldots, e_n$ are the edge variables belonging to the path. For a path containing $n$ edges, the encoding therefore produces $n + 1$ clauses.

One additional clause is added to express that at least one valid path between $s$ and $t$ must exist:

$$x_{p_1} \vee x_{p_2} \vee \cdots \vee x_{p_N}.$$

For hop-constrained reliability, only paths containing at most $k$ edges are considered. In this case, the set $P_{st}$ is restricted to paths satisfying

$$|p| \leq k,$$

where $p$ denotes a simple $s$-$t$ path and $|p|$ represents the number of edges belonging to that path.

The same construction can also be extended to compute the probability that the entire network is connected. In this case, paths are generated for every pair of vertices in the graph. Let

$$Q = \{\{u, v\} \mid u, v \in V(G), u \neq v\}$$

denote the set of all unordered vertex pairs. For every pair $\{u, v\} \in Q$, a set of simple paths $P_{uv}$ is generated and encoded using the same Tseitin construction described above. The network is connected if, for every pair of vertices, at least one valid path exists between them. Therefore, the final formula is given by

$$\Phi_{\text{conn}} = \bigwedge_{\{u,v\} \in Q} \left( \bigvee_{p \in P_{uv}} x_p \right). \tag{5.5}$$

For hop-constrained network reliability, only paths satisfying $|p| \leq k$ are considered.

Let $P_{st}$ denote the set of encoded $s$-$t$ paths. The path-based encoding introduces one auxiliary variable for each path, giving

$$|E| + |P_{st}|$$

variables in total.

Since a path containing $n$ edges contributes $n + 1$ clauses, the total number of clauses is

$$\sum_{p \in P_{st}} (|p| + 1) + 1.$$

For network connectivity, the construction is applied to every unordered vertex pair. The number of variables becomes

$$|E| + \sum_{\{u,v\} \in Q} |P_{uv}|,$$

while the number of clauses is

$$\sum_{\{u,v\} \in Q} \left( \sum_{p \in P_{uv}} (|p| + 1) + 1 \right).$$

Although the number of edges in the graph may remain relatively small, the number of simple paths can grow extremely quickly. For example, a constellation containing 24 nodes and 56 edges can already contain millions of distinct simple $s$-$t$ paths. Therefore, enumerating and encoding all paths may still become computationally expensive for dense graphs or larger constellations.

## 5.3. Projected Weighted Model Counting

To compute reliability metrics from the propositional encodings described in the previous sections, we use Projected Weighted Model Counting (PWMC). Each communication edge is represented by a Boolean variable whose literal weights correspond to the probability that the communication link exists or fails. Auxiliary variables introduced by the encodings are not associated with probabilities and are therefore excluded from the projection.

For a given reliability property, such as the existence of a path between two ground-connected satellites or network connectivity, we construct a propositional formula. The projected weighted model count of this formula then yields the probability that the property holds.

For example, Equation 5.1 defines a formula that is satisfied whenever no communication path exists between two nodes $s$ and $t$. PWMC computes the probability that this formula is satisfied. Similarly, the formulas introduced in the previous section can be used to compute the probabilities of hop-constrained communication and network connectivity.

# 6

# Experiments & Results

In this chapter, we present the experiments designed to evaluate the communication reliability of Earth–Moon satellite constellations. The experiments address the following research questions:

**Q1** How does communication reliability vary over time in Earth–Moon satellite constellations?

**Q2** How does limiting the maximum number of communication relays through a hop constraint $k$ affect communication reliability?

**Q3** How do the path-based and reachability-based propositional encodings compare in terms of CNF size and Ganak solving time?

**Q4** How does the constellation configuration affect communication reliability?

The results show that the communication reliability varies over time and is influenced by the constellation geometry. Increasing the hop limit generally improves communication reliability, which is more visible in larger constellations. The comparison of the propositional encodings shows that the path-based encoding performs well for small hop limits, while the reachability-based encoding scales better as the hop limit and constellation size increase. Larger constellation configurations generally achieve higher communication reliability, although constellation geometry and the distribution of satellites across orbital planes also influence performance.

The chapter begins by describing the experimental setup, covering the constellation configurations used, the selection of time windows for computation, and the computational environment. It then presents and discusses the experimental results.

## 6.1. Experimental Setup

This section presents the experimental setup used to evaluate the proposed reliability framework. It describes the constellation configurations, time discretisation strategy, and computational environment used throughout the experiments.

### 6.1.1. Constellation configurations

To investigate both reliability and scalability, we consider several Earth–Moon constellation configurations of varying size and complexity. The configurations differ in the number of satellites, orbital planes, and ground-connected and long-range satellites. By varying these characteristics, we can analyse how constellation design influences communication reliability and computational complexity.

All configurations use an Earth inclination of 30°, a Moon inclination of 45°, a Walker phase parameter $f = 1$, and an orbital altitude of 275 km. These parameters are kept constant throughout the experiments to isolate the impact of constellation size and satellite role distribution. Table 6.1 summarises the Earth–Moon constellation configurations used throughout the experiments.

**Table 6.1:** Earth–Moon constellation configurations used in the experiments. GC denotes ground-connected satellites and LR denotes long-range satellites.

| Configuration | Earth | | | | Moon | | | |
|---|---|---|---|---|---|---|---|---|
| | $t$ | $p$ | GC | LR | $t$ | $p$ | GC | LR |
| C0 | 10 | 2 | 3 | 3 | 10 | 2 | 3 | 3 |
| C1 | 12 | 2 | 4 | 3 | 12 | 2 | 4 | 3 |
| C2 | 12 | 3 | 4 | 3 | 12 | 3 | 4 | 3 |
| C3 | 18 | 3 | 4 | 4 | 18 | 3 | 4 | 4 |
| C4 | 12 | 2 | 4 | 3 | 18 | 3 | 4 | 4 |
| C5 | 18 | 3 | 4 | 4 | 12 | 2 | 4 | 3 |
| C6 | 24 | 4 | 5 | 4 | 24 | 4 | 5 | 4 |

### 6.1.2. Time discretisation

To study the evolution of the communication network over time, each constellation is evaluated at multiple discrete timestamps. The timestamps are chosen to capture meaningful changes in the satellite geometry and communication topology. To determine an appropriate duration for the experiments, we first estimate the orbital periods of the Earth and the Moon constellations. The orbital periods of the satellites are estimated using Kepler's third law:

$$T = 2\pi\sqrt{\frac{a^3}{\mu}}. \tag{6.1}$$

where $T$ denotes the orbital period, $a$ is the semi-major axis of the orbit, and $\mu$ is the gravitational parameter of the central body.

For the Earth constellation, using the Earth radius $R_E = 6378.137\,\text{km}$, the semi-major axis becomes

$$a_E = 6378.137 + 275 = 6653.137\,\text{km}. \tag{6.2}$$

Using the Earth's gravitational parameter $\mu_E = 398600.4418\,\text{km}^3/\text{s}^2$, the orbital period is calculated as:

$$T_E = 2\pi\sqrt{\frac{6653.137^3}{398600.4418}} \approx 5400\,\text{s} \approx 90\,\text{minutes}. \tag{6.3}$$

Similarly, the Moon satellites orbit at an altitude of 275 km. Using the Moon radius $R_M = 1737.4\,\text{km}$, the semi-major axis becomes

$$a_M = 1737.4 + 275 = 2012.4\,\text{km}. \tag{6.4}$$

Using the Moon's gravitational parameter $\mu_M = 4902.800066\,\text{km}^3/\text{s}^2$, the orbital period is calculated as:

$$T_M = 2\pi\sqrt{\frac{2012.4^3}{4902.800066}} \approx 8100\,\text{s} \approx 135\,\text{minutes}. \tag{6.5}$$

The Moon itself also revolves around the Earth. Using the average Earth–Moon distance $a_{EM} = 384400\,\text{km}$, the orbital period becomes

$$T_{EM} = 2\pi\sqrt{\frac{384400^3}{398600.4418}} \approx 2.36 \times 10^6\,\text{s} \approx 27.3\,\text{days}. \tag{6.6}$$

This period is significantly larger than the orbital periods of both the Earth and the Moon satellites. Therefore, over the time interval considered in this thesis, the Moon's position relative to the Earth changes only slightly and has a limited impact on the communication topology.

The Earth and Moon satellite orbital periods are approximately 90 minutes and 135 minutes, respectively. A near common multiple is approximately 4 hours and 30 minutes, since 3 Earth-satellite revolutions correspond to $3 \cdot 90 \approx 270$ minutes, while 2 Moon-satellite revolutions correspond to $2 \cdot 135 \approx 270$ minutes. Therefore, the relative constellation geometry is expected to become similar again after roughly 4.5 hours. Based on this observation, each constellation is evaluated at 10 uniformly distributed timestamps over a 4.5-hour interval. This choice captures the short-term evolution of the communication topology while remaining computationally feasible.

### 6.1.3. Experiment design

All experiments were executed on the DelftBlue supercomputer. Each reliability evaluation for a constellation was submitted as an independent batch job and executed in a Python environment together with the Ganak projected weighted model counter. Every job was allocated 4 CPU cores and 15.6 GB of memory. Depending on the complexity of the reliability computation, based on the constellation size, reliability metric, and hop constraint, runtime limits of 3, 8, or 24 hours were used. For individual Ganak calls, we used a timeout of 5 minutes. This made it possible to compute the source–target probabilities for one constellation and one hop limit within the 24-hour job limit. We also tested a 15-minute Ganak timeout for several instances. However, most instances either finished within 5 minutes or did not finish even with the longer timeout.

We implemented all experiments in Python 3.11. We performed satellite propagation using PyKep 2.6, an astrodynamics library developed by the European Space Agency (ESA) [39]. We used the igraph library for graph operations. For projected weighted model counting, we used Ganak [36, 37], an exact model counter that achieves substantial performance improvements compared to other state-of-the-art model-counting tools.

For the path-based encoding, we generated the Tseitin-style encoding manually. During development, we also experimented with the `to_cnf` function provided by the SymPy library, but this approach did not scale to the larger instances considered in this thesis. We translated all propositional formulas into DIMACS CNF format, the standard input format supported by Ganak.

The source code used for all experiments is publicly available at

`https://github.com/roxanabacalie/satellite-constellation`

All results reported in this thesis were generated using commit `82aeedc` of the repository.

## 6.2. Results

In this section, we present the experimental results for the reliability metrics introduced in section 4.3. We analyse how these probabilities evolve over time, how hop constraints affect communication reliability, and how the proposed encodings compare in terms of Ganak solving time, number of CNF clauses and number of variables.

For the connected-network probability without a hop constraint, neither encoding produced results within the available time. The path-based encoding runs were terminated by the SLURM out-of-memory handler before completion. This happens during CNF construction, because representing all simple paths in the network requires a large number of auxiliary variables that grows rapidly with graph size. The reachability-based encoding is not limited by memory, but exceeds the Ganak timeout for all tested configurations. Therefore, the connected-network probability with no hop constraint is computationally infeasible for the constellation sizes considered, regardless of the encoding used. However, the reachability-based encoding is the more promising option, as it is not limited by memory and may complete successfully with a longer timeout.

For the hop-constrained connected-network probability computation, we only evaluated the path-based encoding. A reachability-based formulation would require additional layered reachability variables and constraints for all node pairs, substantially increasing the size of the encoding. The resulting

probabilities were close to zero for all completed instances. Since these values provide limited additional insight beyond the pairwise communication analysis, we focus the remainder of this chapter on the communication probability between pairs of ground-connected satellites orbiting the Earth and the Moon.

### 6.2.1. Q1: Reliability over time

Figures 6.1, 6.2 and 6.3 show the communication probability between Earth and Moon ground-connected satellite pairs over time for three constellation configurations of increasing size: C1 with 12 satellites around each celestial body, C5 with 18 Earth satellites and 12 Moon satellites, and C6 with 24 satellites around each celestial body. We provide a detailed description of these configurations in Table 6.1. In the figures, labels such as `E-P1-S0` and `M-P0-S0` denote satellites in specific orbital planes and positions within that plane around the Earth and the Moon, respectively. For example, `E-P1-S3` corresponds to satellite 3 in orbital plane 1 around Earth.

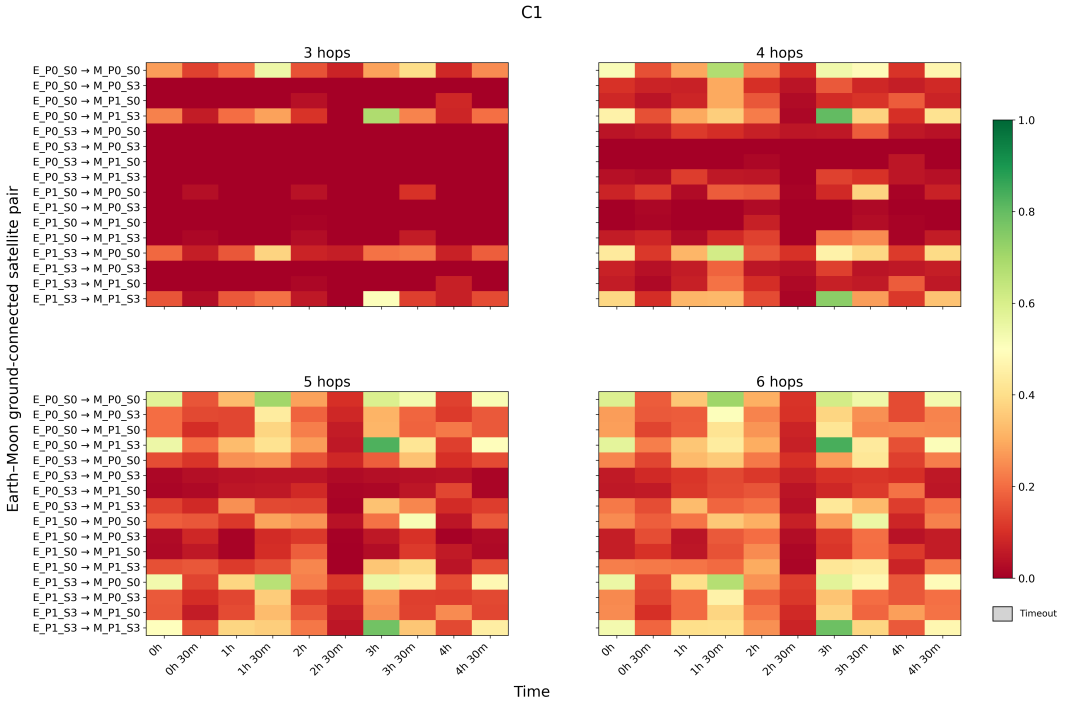


**Figure 6.1:** Probability that a communication path of at most $k$ hops exists between each Earth–Moon ground-connected satellite pair over time for constellation C1. Results are computed using the reachability-based encoding, with path-based results used only when no reachability-based result is available.

In the figure, grey cells indicate instances for which the probability could not be computed within the allocated computational budget. A first observation is that communication patterns at timestamps 0 h and 4 h 30 min are similar, which is consistent with the approximate common multiple of the Earth and Moon satellite orbital periods discussed. We can still observe small differences, for instance in constellation C5, since the common multiple is only an approximation, and the Moon's movement slightly changes the geometry over time.

For all evaluated constellation configurations, communication probabilities between ground-connected satellite pairs vary significantly over time as satellites move along their orbits. As inter-satellite distances change, so do the probabilities assigned to communication links, causing timestamps of stronger connectivity to alternate with timestamps of weaker connectivity. Several timestamps consistently show lower communication probabilities across all three configurations. The figures show noticeably lower reliability at times 30 min, 2 h 30 min and 4 h. These timestamps coincide with a reduced number of long-range communication links between the Earth and the Moon constellations. Figure 6.4 illustrates this for the timestamp at 30 min. At this time, configurations C1 and C5 contain only two Earth–Moon long-range links, while C6 contains six. Although C6 has more long-range links, this is still fewer than

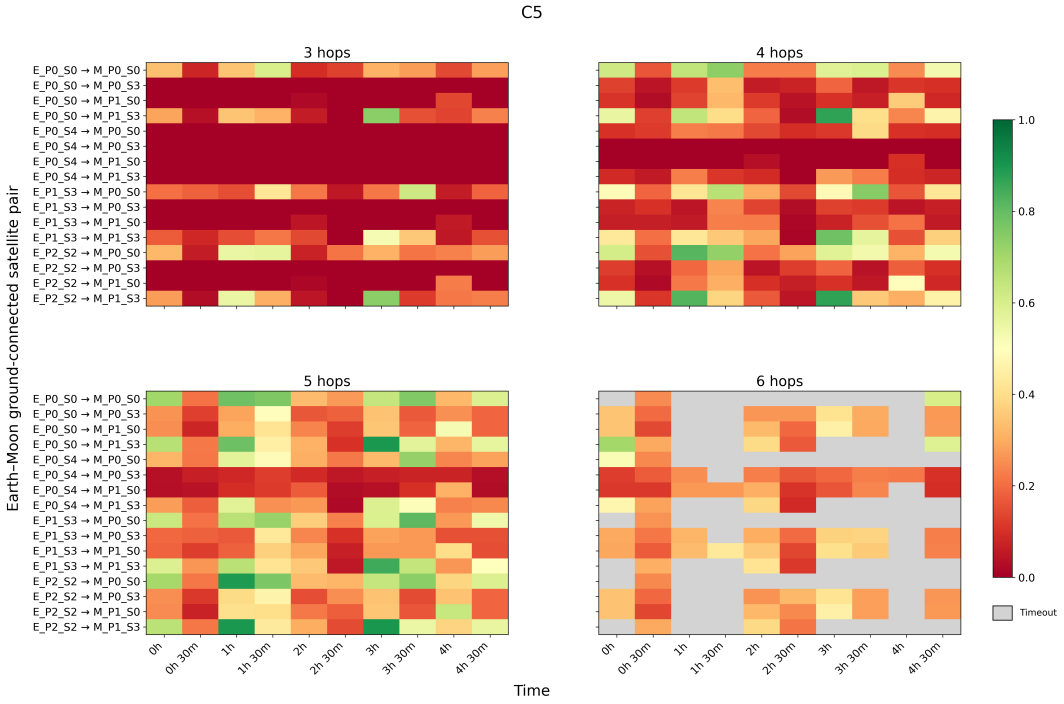


**Figure 6.2:** Probability that a communication path of at most $k$ hops exists between each Earth–Moon ground-connected satellite pair over time for constellation C5. Results are computed using the reachability-based encoding, with path-based results used only when no reachability-based result is available.

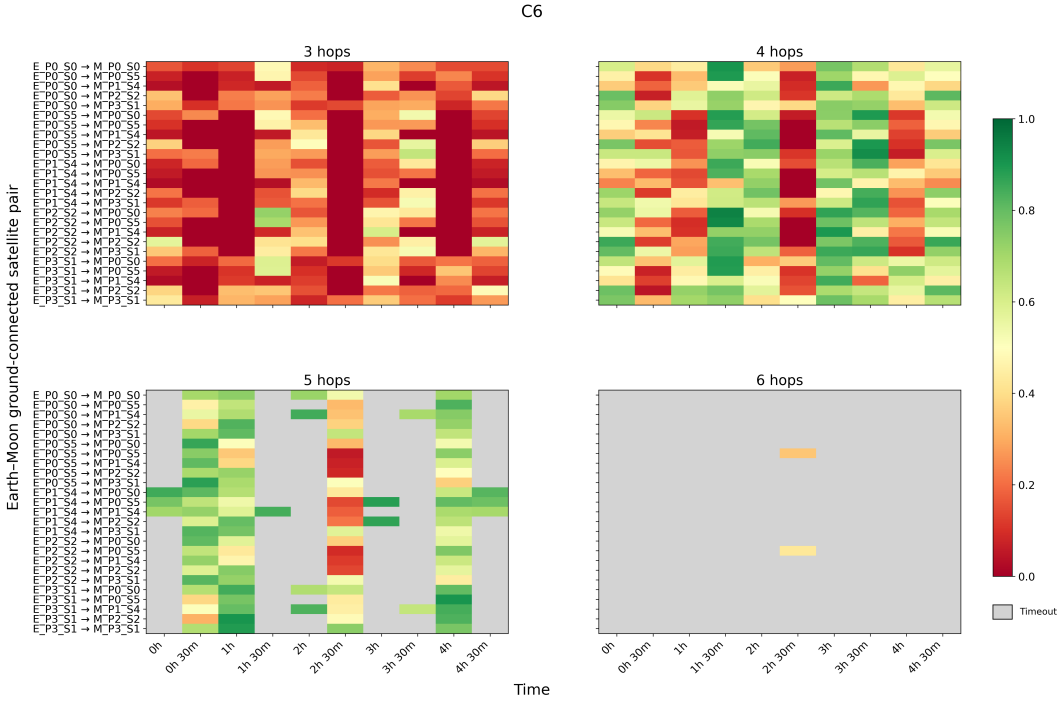


**Figure 6.3:** Probability that a communication path of at most $k$ hops exists between each Earth–Moon ground-connected satellite pair over time for constellation C6. Results are computed using the reachability-based encoding, with path-based results used only when no reachability-based result is available.

at timestamps associated with higher communication reliability.

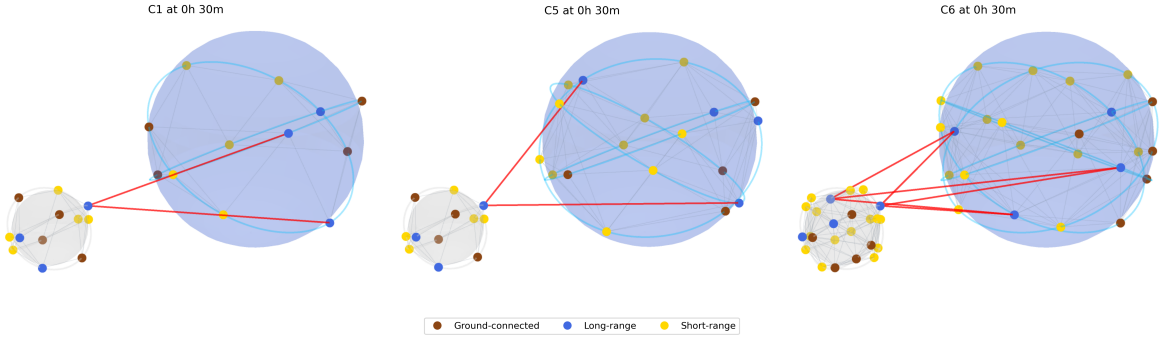


**Figure 6.4:** Constellation configurations C1, C5 and C6 at 30 min. Earth–Moon long-range communication links are highlighted in red.

The results also show that communication reliability is not uniform across satellite pairs. For example, in constellation C1, pairs such as `EP0S0-MP0S0`, `EP0S0-MP1S3`, `EP1S3-MP0S0`, and `EP1S3-MP1S3` achieve higher communication probabilities, while other pairs remain unreliable throughout most of the observation period.

### 6.2.2. Q2: Effect of hop constraints

We can observe the impact of hop constraints on reliability in Figures 6.1, 6.2, and 6.3 from the previous section. Increasing the hop limit generally improves communication reliability, since allowing additional hops enables longer communication paths and increases the probability that at least one path exists between a given Earth–Moon satellite pair.

The extent of this improvement depends on the constellation configuration. In constellation C1, the increase in communication probability is relatively small, and several satellite pairs remain unreliable even for larger hop limits. Constellation C6 shows a larger increase in communication probability when the hop limit is increased, especially between $k = 3$ and $k = 4$. This happens because the constellation is larger, resulting in longer communication paths.

### 6.2.3. Q3: Comparison of propositional encodings

We compare the reachability-based and path-based encodings in terms of computational performance for the communication probability computation between pairs of ground-connected satellites orbiting the Earth and the Moon, as this is the only setting in which results from both encodings are available. We compare the two approaches using three metrics: Ganak solving time, number of CNF variables, and number of CNF clauses.

Table 6.2 shows the fraction of completed probability computations between Earth and Moon ground-connected satellite pairs. For $k = 3$, both encodings completed all computations for all constellation configurations. For $k = 6$, completion rates decrease for the larger constellations. The reachability-based encoding completed a larger fraction of instances than the path-based encoding, suggesting it scales better as constellation size and hop limit increase.

Figure 6.5 compares the Ganak solving times of the reachability-based and path-based encodings for $k = 3$ and $k = 6$. For $k = 3$, most points lie above the diagonal, meaning the path-based encoding is faster to solve in most cases. However, the solving times are very small for both encodings. For $k = 6$, points are more evenly spread on the diagonal, and the reachability-based encoding is faster for a larger number of instances. Therefore, as the hop limit increases, the reachability-based encoding becomes more efficient in terms of Ganak solving time.

Figure 6.6 compares the CNF model size produced by the two encodings in terms of the number of clauses and number of variables. For $k = 3$, all points lie above the diagonal in both the clauses and variables plots, meaning the reachability-based encoding produces larger CNF formulas than the path-based encoding, which explains the smaller Ganak solving times observed for the path-based encoding at $k = 3$.

**Table 6.2:** Fraction of completed probability computations between Earth and Moon ground-connected satellite pairs.

| | $k = 3$ | | $k = 6$ | |
|---|---|---|---|---|
| Constellation | Path-based | Reachability-based | Path-based | Reachability-based |
| C0 | 100.0% | 100.0% | 80.0% | 100.0% |
| C1 | 100.0% | 100.0% | 97.5% | 100.0% |
| C2 | 100.0% | 100.0% | 100.0% | 100.0% |
| C3 | 100.0% | 100.0% | 6.9% | 15.6% |
| C4 | 100.0% | 100.0% | 36.9% | 54.4% |
| C5 | 100.0% | 100.0% | 35.6% | 52.5% |
| C6 | 100.0% | 100.0% | 0.0% | 0.8% |

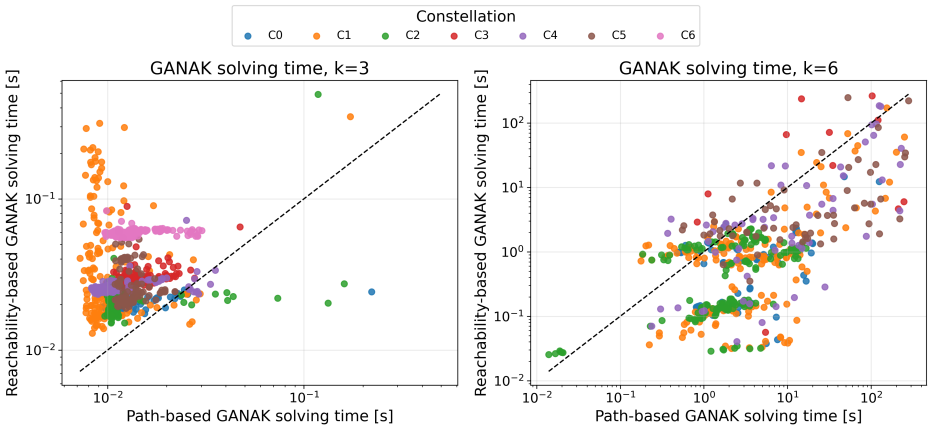


**Figure 6.5:** Comparison of GANAK solving times for the path-based and reachability-based encodings on a logarithmic scale. Each point represents a ground-connected satellite pair at a given timestamp. Only instances solved by both encodings are shown.

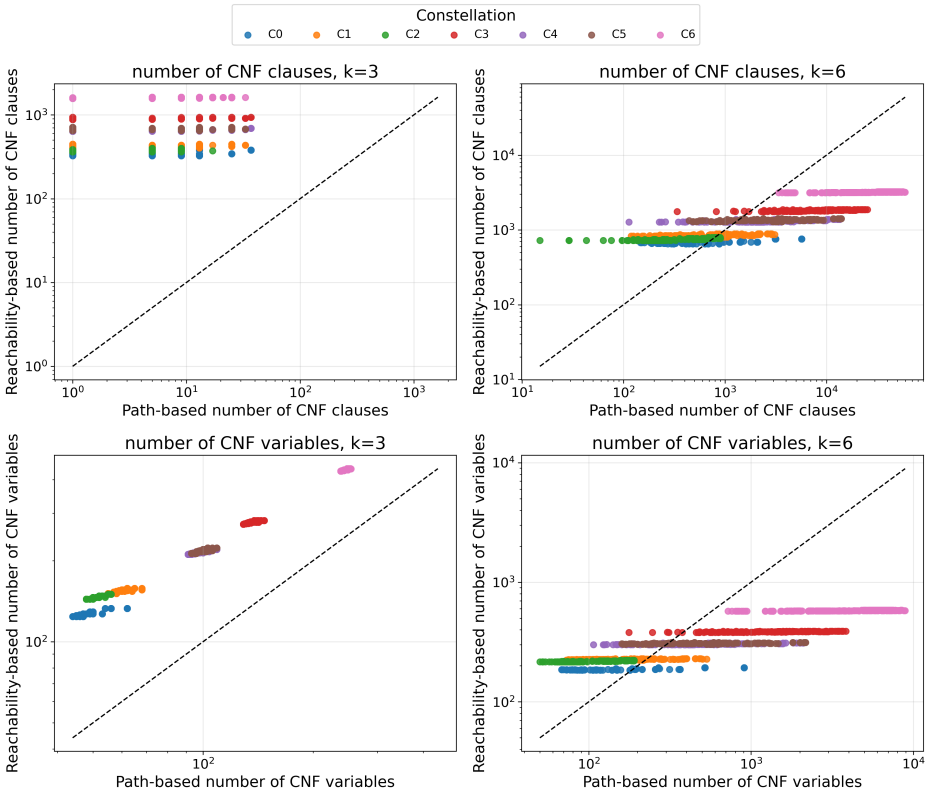


**Figure 6.6:** Comparison of CNF model size for the path-based and reachability-based encodings on a logarithmic scale. Each point represents a ground-connected satellite pair at a given timestamp.

For $k = 6$, most points in the clauses plot fall below the diagonal, and the variables plot shows the same trend: the reachability-based encoding uses fewer variables for most instances, which becomes more pronounced for larger constellations. This helps explain why the reachability-based encoding becomes faster to solve at larger hop limits, as observed earlier.

Overall, the CNF size comparison reinforces the Ganak solving time results: the path-based encoding produces more compact formulas at small hop limits, but the reachability-based encoding becomes the more scalable option for larger constellations and higher hop limits.

### 6.2.4. Q4: Influence of constellation configuration

Given the large number of unfinished computations for $k = 6$, we focus this section on hop limits $k = 3$ and $k = 5$. Figure 6.7 compares the distribution of communication probabilities between Earth–Moon ground-connected satellite pairs for the evaluated constellation configurations. Each box summarises all completed probability computations across all considered timestamps and satellite pairs.

For $k = 3$, communication probabilities are generally low across all evaluated constellations. Although some high-probability instances exist, the median probability remains close to zero for most configurations. Constellations C3 and C6 have higher probability values than the smaller configurations, suggesting that larger constellations have a more reliable communication even under restrictive hop limits. For $k = 5$, the distributions shift upwards for all constellation configurations. Constellations C3 and C6 achieve the highest median probabilities and the largest concentration of high-probability instances.

Therefore, the results show that constellation size is an important factor, as larger constellations generally achieve higher communication probabilities. Comparing C1 and C2 suggests that distributing satellites across more orbital planes can improve communication reliability. Overall, constellation geometry plays an important role alongside constellation size in determining communication reliability.

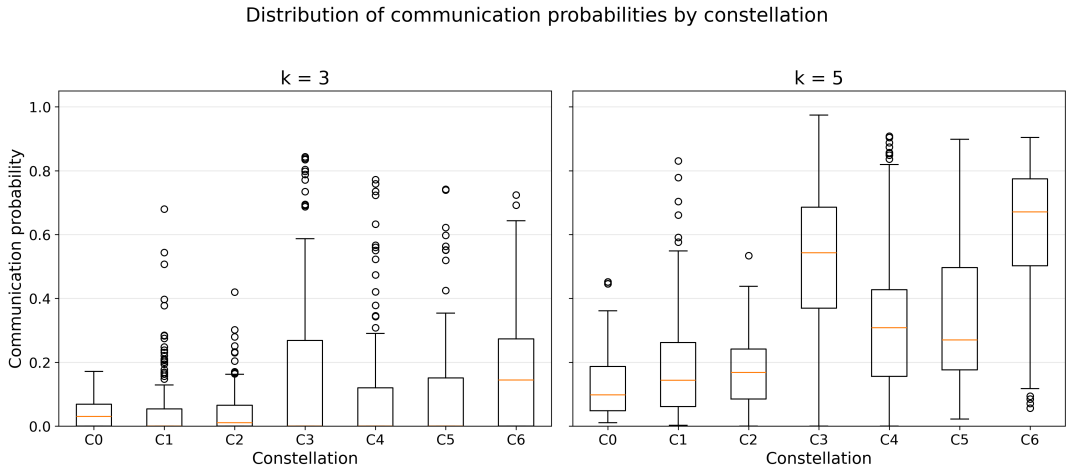


**Figure 6.7:** Distribution of communication probabilities between Earth–Moon ground-connected satellite pairs. Each box summarises all computed probabilities across evaluated timestamps and satellite pairs.

# 7

# Conclusion & Future Work

## 7.1. Conclusion

In this thesis, we investigated how the communication reliability of Earth–Moon satellite constellations can be modelled and evaluated using projected weighted model counting. We modelled Earth–Moon satellite constellations as probabilistic graphs, where communication links are assigned probabilities based on the distances between satellites. We considered two reliability metrics: the probability that communication exists between an Earth and Moon ground-connected satellite pair and the probability that the overall network is connected. To evaluate these metrics, we adapted the reachability-based encoding from the literature, which models connectivity through reachability variables and constraints, and implemented a path-based encoding that explicitly represents communication paths between satellites. We also extended both approaches to support hop-constrained reliability to account for scenarios in which the number of satellite relays is limited.

Our experiments show that the communication probability between ground-connected satellites can be evaluated successfully for the considered constellation configurations. In contrast, the connected-network probability computation proved to be more challenging. For the case without a hop constraint, neither encoding was able to compute this metric within the available computational budget. For the hop-constrained case, the computed connected-network probabilities were very close to zero, showing that maintaining connectivity between all satellites becomes highly unlikely under the considered constellation configurations and hop limits.

The results further illustrate that communication reliability varies over time as satellites move along their orbits and as the geometry of the constellation changes. Increasing the hop limit generally improves communication reliability. The constellation configuration also influences communication reliability, with larger configurations achieving higher communication probabilities than others. The comparison of the two propositional encodings shows that the path-based encoding performs well for small hop limits, while the reachability-based encoding scales better as the hop limit and constellation size increase. For larger instances, the reachability-based encoding completes a larger fraction of computations within the available computational budget.

The results presented in this thesis depend on several simplifying assumptions. We assumed a fixed Earth-centred reference frame, modelled communication probabilities as a function of the distance between satellites, and assumed continuous communication between ground-connected satellites and their associated ground stations. These assumptions allowed us to focus on the reliability evaluation problem and the effects of constellation geometry and orbital motion, while abstracting away from the more detailed astrodynamics considerations.

Overall, this thesis shows that projected weighted model counting can be used to evaluate communication reliability in Earth–Moon satellite constellations and provides a foundation for future research on the modelling, analysis, and design of reliable lunar communication networks.

## 7.2. Future Work

A promising direction for future work is to extend the proposed reliability evaluation framework to support constellation design and optimisation. Rather than evaluating a fixed set of constellation configurations, future work could investigate how to minimise the number of deployed satellites while maintaining a required level of communication reliability between the Earth and the Moon. This problem can be formulated as a stochastic constraint optimisation problem. The reliability models developed in this thesis could be combined with existing techniques for stochastic constraint optimisation [40, 41, 42, 43, 44].

A second direction for future work is to address the scalability limitations encountered in this thesis. While exact projected weighted model counting provides accurate reliability estimates, several larger instances could not be solved within the available computational budget. Future work could investigate approximate reliability estimation techniques based on knowledge compilation, decision diagrams, or bounded reliability computations that provide upper and lower bounds on the communication reliability.

Future work could also consider longer evaluation periods. While the experiments in this thesis focus on a time window of several hours, modelling constellation behaviour over days or weeks would provide a more comprehensive assessment of communication reliability over time.

# References


[1] S. C. Casanova. "Overview of ispace-EUROPE's Upcoming Lunar Rover Mission: Tenacious". In: *56th Lunar and Planetary Science Conference*. Vol. 3090. LPI Contributions. Mar. 2025, 1746, p. 1746.

[2] NASA. *Artemis*. https://www.nasa.gov/humans-in-space/artemis/. Accessed: 2026-02-06. 2026.

[3] European Space Agency. *ESA's Moonlight Programme: Pioneering the Path for Lunar Exploration*. Accessed: 2026-06-04. 2024. URL: https://www.esa.int/Applications/Connectivity_and_Secure_Communications/ESA_s_Moonlight_programme_Pioneering_the_path_for_lunar_exploration.

[4] Vaida Karaliunaite. *How Many Satellites are in Space? - NanoAvionics — nanoavionics.com*. https://nanoavionics.com/blog/how-many-satellites-are-in-space/. [Accessed 04-06-2026].

[5] Chenyu Wu et al. "Enhancing LEO Mega-constellations with Inter-Satellite Links: Vision and Challenges". In: *IEEE Wireless Communications* 32.5 (2025), pp. 196–202. DOI: 10.1109/MWC.003.2400195.

[6] Georgi Gary Rozenman et al. *Free-space and Satellite-Based Quantum Communication: Principles, Implementations, and Challenges*. 2026. DOI: 10.48550/ARXIV.2602.01426. URL: https://arxiv.org/abs/2602.01426.

[7] H.-J. Briegel et al. "Quantum Repeaters: The Role of Imperfect Local Operations in Quantum Communication". In: *Phys. Rev. Lett.* 81 (26 1998), pp. 5932–5935. DOI: 10.1103/PhysRevLett.81.5932. URL: https://link.aps.org/doi/10.1103/PhysRevLett.81.5932.

[8] Max Bannach, Giacomo Acciarini, and Dario Izzo. *Reliability of Constellations with Inter-Satellite Communication*. eng. Milan, 2024.

[9] Roger R. Bate, Donald D. Mueller, and Jerry E. White. *Fundamentals of Astrodynamics*. New York: Dover Publications, 1971.

[10] J.R. Wertz and W. Larson. *Space Mission Analysis and Design*. Space Technology Library. Springer Netherlands, 1999. ISBN: 9780792359012. URL: https://books.google.nl/books?id=QJanyiWfvXMC.

[11] John G. Walker. "Satellite constellations". In: *Journal of the British Interplanetary Society* 37 (1984), p. 559.

[12] Lasunncty. *Keplerian orbital elements*. Wikimedia Commons. CC BY-SA 3.0. 2010. URL: https://commons.wikimedia.org/wiki/File:Keplerian_orbit_elements.png.

[13] Mordechai Ben-Ari. *Mathematical logic for computer science*. Springer Science & Business Media, 2012.

[14] Armin Biere et al., eds. *Handbook of Satisfiability - Second Edition*. Vol. 336. Frontiers in Artificial Intelligence and Applications. IOS Press, 2021. ISBN: 978-1-64368-160-3. DOI: 10.3233/FAIA336. URL: https://doi.org/10.3233/FAIA336.

[15] Stephen A. Cook. "The complexity of theorem-proving procedures". In: *Proceedings of the Third Annual ACM Symposium on Theory of Computing*. STOC '71. Shaker Heights, Ohio, USA: Association for Computing Machinery, 1971, pp. 151–158. ISBN: 9781450374644. DOI: 10.1145/800157.805047. URL: https://doi.org/10.1145/800157.805047.

[16] G. S. Tseitin. "On the Complexity of Derivation in Propositional Calculus". In: *Automation of Reasoning: 2: Classical Papers on Computational Logic 1967–1970*. Ed. by Jörg H. Siekmann and Graham Wrightson. Berlin, Heidelberg: Springer Berlin Heidelberg, 1983, pp. 466–483. ISBN: 978-3-642-81955-1. DOI: 10.1007/978-3-642-81955-1_28. URL: https://doi.org/10.1007/978-3-642-81955-1_28.

[17] David S. Johnson and Michael A. Trick, eds. *Cliques, Coloring, and Satisfiability*. Vol. 26. DIMACS Series in Discrete Mathematics and Theoretical Computer Science. American Mathematical Society, 1996. ISBN: 9781470439842. DOI: 10.1090/dimacs/026. URL: http://dx.doi.org/10.1090/dimacs/026.

[18] Leslie G. Valiant. "The complexity of enumeration and reliability problems". In: *SIAM Journal on Computing* 8.3 (1979), pp. 410–421.

[19] Michael O. Ball. "Computational Complexity of Network Reliability Analysis: An Overview". In: *IEEE Transactions on Reliability* 35.3 (1986), pp. 230–239. ISSN: 0018-9529. DOI: 10.1109/tr.1986.4335422. URL: http://dx.doi.org/10.1109/TR.1986.4335422.

[20] Israel Leyva-Mayorga, Beatriz Soret, and Petar Popovski. "Inter-Plane Inter-Satellite Connectivity in Dense LEO Constellations". In: *IEEE Transactions on Wireless Communications* 20.6 (2021), pp. 3430–3443. ISSN: 1558-2248. DOI: 10.1109/twc.2021.3050335. URL: http://dx.doi.org/10.1109/TWC.2021.3050335.

[21] Yonghwa Lee and Jihwan Choi. "Connectivity Analysis of Mega Constellation Satellite Networks with Optical Inter-Satellite Links". In: *IEEE Transactions on Aerospace and Electronic Systems* PP (June 2021), pp. 1–1. DOI: 10.1109/TAES.2021.3090914.

[22] Radhika Radhakrishnan et al. *Survey of Inter-satellite Communication for Small Satellite Systems: Physical Layer to Network Layer View*. 2016. arXiv: 1609.08583 [cs.NI]. URL: https://arxiv.org/abs/1609.08583.

[23] Ruibo Wang, Mustafa A. Kishk, and Mohamed-Slim Alouini. *Reliability Analysis of Multi-hop Routing in Multi-tier LEO Satellite Networks*. 2023. arXiv: 2303.02286 [cs.NI]. URL: https://arxiv.org/abs/2303.02286.

[24] Leonardo Dueñas-Osorio, Moshe Vardi, and Javier Rojo. "Quantum-inspired Boolean states for bounding engineering network reliability assessment". In: *Structural Safety* 75 (Nov. 2018), pp. 110–118. DOI: 10.1016/j.strusafe.2018.05.004.

[25] Gary Hardy, Corinne Lucet, and Nikolaos Limnios. "K-Terminal Network Reliability Measures With Binary Decision Diagrams". In: *Reliability, IEEE Transactions on* 56 (Oct. 2007), pp. 506–515. DOI: 10.1109/TR.2007.898572.

[26] D. Levinson, H.X. Liu, and M. Bell. *Network Reliability in Practice: Selected Papers from the Fourth International Symposium on Transportation Network Reliability*. Transportation Research, Economics and Policy. Springer New York, 2011. ISBN: 9781461409472. URL: https://books.google.nl/books?id=Q2_7uVHr3QYC.

[27] Johannes U. Herrmann and Sieteng Soh. "A memory efficient algorithm for network reliability". In: *2009 15th Asia-Pacific Conference on Communications*. IEEE, Oct. 2009, 171, p. 171. DOI: 10.1109/APCC.2009.5375505.

[28] Roger Paredes et al. "Principled network reliability approximation: A counting-based approach." In: (Nov. 2019).

[29] Roger Paredes et al. "A Weighted Model Counting Approach for Critical Infrastructure Reliability". In: May 2019. DOI: 10.22725/ICASP13.383.

[30] Leonardo Duenas-Osorio et al. "Counting-Based Reliability Estimation for Power-Transmission Grids". In: *Proceedings of the AAAI Conference on Artificial Intelligence* 31.1 (2017). DOI: 10.1609/aaai.v31i1.11178. URL: https://ojs.aaai.org/index.php/AAAI/article/view/11178.

[31] Xin Xu, Zhixiang Gao, and Aijun Liu. "Robustness of satellite constellation networks". In: *Computer Communications* 210 (2023), pp. 130–137. ISSN: 0140-3664. DOI: https://doi.org/10.1016/j.comcom.2023.07.036. URL: https://www.sciencedirect.com/science/article/pii/S0140366423002694.

[32] Johannes K. Fichte, Markus Hecher, and Florim Hamiti. "The Model Counting Competition 2020". In: *ACM Journal of Experimental Algorithmics* 26 (Oct. 2021), pp. 1–26. ISSN: 1084-6654. DOI: 10.1145/3459080. URL: http://dx.doi.org/10.1145/3459080.

[33] Johannes K. Fichte et al. *Solving Projected Model Counting by Utilizing Treewidth and its Limits*. 2023. arXiv: 2305.19212 [cs.CC]. URL: https://arxiv.org/abs/2305.19212.

[34] Max Bannach and Markus Hecher. *Structure-Guided Automated Reasoning*. 2025. arXiv: 2312.14620 [cs.LO]. URL: https://arxiv.org/abs/2312.14620.

[35] Jeffrey Dudek, Vu Phan, and Moshe Vardi. "ADDMC: Weighted Model Counting with Algebraic Decision Diagrams". In: *Proceedings of the AAAI Conference on Artificial Intelligence* 34.02 (2020), pp. 1468–1476. DOI: 10.1609/aaai.v34i02.5505. URL: https://ojs.aaai.org/index.php/AAAI/article/view/5505.

[36] Shubham Sharma et al. "GANAK: A Scalable Probabilistic Exact Model Counter". In: *Proceedings of the Twenty-Eighth International Joint Conference on Artificial Intelligence*. IJCAI-2019. International Joint Conferences on Artificial Intelligence Organization, Aug. 2019, pp. 1169–1176. DOI: 10.24963/ijcai.2019/163. URL: http://dx.doi.org/10.24963/ijcai.2019/163.

[37] Mate Soos and Kuldeep S. Meel. "Engineering an Efficient Probabilistic Exact Model Counter". In: *Computer Aided Verification*. Springer Nature Switzerland, 2025, pp. 72–91. ISBN: 9783031986826. DOI: 10.1007/978-3-031-98682-6_5. URL: http://dx.doi.org/10.1007/978-3-031-98682-6_5.

[38] J. Greiner et al. "A proposed network of gamma-ray burst detectors on the global navigation satellite systemGalileoG2". In: *Astronomy & Astrophysics* 664 (Aug. 2022), A131. ISSN: 1432-0746. DOI: 10.1051/0004-6361/202142835. URL: http://dx.doi.org/10.1051/0004-6361/202142835.

[39] Dario Izzo et al. *esa/pykep: Optimize*. Version v2.6. Oct. 2020. DOI: 10.5281/zenodo.4091753. URL: https://doi.org/10.5281/zenodo.4091753.

[40] Anna Louise D. Latour, Behrouz Babaki, and Siegfried Nijssen. "Stochastic Constraint Propagation for Mining Probabilistic Networks". In: *Proceedings of the Twenty-Eighth International Joint Conference on Artificial Intelligence, IJCAI-19*. International Joint Conferences on Artificial Intelligence Organization, July 2019, pp. 1137–1145. DOI: 10.24963/ijcai.2019/159. URL: https://doi.org/10.24963/ijcai.2019/159.

[41] Anna L.D. Latour et al. "Exact stochastic constraint optimisation with applications in network analysis". In: *Artificial Intelligence* 304 (2022), p. 103650. ISSN: 0004-3702. DOI: https://doi.org/10.1016/j.artint.2021.103650. URL: https://www.sciencedirect.com/science/article/pii/S0004370221002010.

[42] Anna L. D. Latour et al. "Combining Stochastic Constraint Optimization and Probabilistic Programming. From Knowledge Compilation to Constraint Solving". In: *Principles and Practice of Constraint Programming (CP 2017)*. Vol. 10416. Lecture Notes in Computer Science. Springer, 2017, pp. 495–511. ISBN: 978-3-319-66157-5. DOI: 10.1007/978-3-319-66158-2_32.

[43] Anna L. D. Latour. "Optimal Decision-Making Under Constraints and Uncertainty". PhD thesis. Leiden University, 2022. URL: https://hdl.handle.net/1887/3455662.

[44] Anna L. D. Latour et al. *The Cardinality of Identifying Code Sets for Soccer Ball Graph with Application to Remote Sensing*. 2024. arXiv: 2407.14120 [cs.AI]. URL: https://arxiv.org/abs/2407.14120.

# A

# Declaration of Generative AI Use

I used generative AI tools during the research, implementation, and writing phases of this thesis in accordance with the TU Delft guidelines on the responsible use of AI in academic work.

I used the following AI tools: Grammarly (`https://app.grammarly.com/`) for grammar, spelling, and fluency improvements, ChatGPT (`https://chatgpt.com/`) and Claude (`https://claude.ai`) for writing assistance, LaTeX formatting, code review, and thesis structure, and GitHub Copilot (`https://github.com/features/copilot`) for inline code suggestions during implementation. I did not upload any sensitive, confidential, or proprietary data to any of these tools during the preparation of this thesis.

## A.1. AI Usage during research

During the research phase, I used generative AI to assist with brainstorming research questions and experiment ideas, clarifying concepts related to network reliability, propositional logic, projected weighted model counting, graph theory, and orbital mechanics, and identifying relevant keywords and topics for literature searches.

I used AI-generated explanations only as a starting point for understanding. I verified all concepts, claims, explanations, and summaries against the original academic papers, textbooks, and official documentation referenced in this thesis. To guard against plagiarism, I searched for supporting academic sources whenever AI tools suggested claims, concepts, or research directions, and I evaluated their relevance and correctness. I also discussed ideas with my thesis supervisors.

## A.2. AI usage during implementation

During the implementation phase, I used generative AI to assist with debugging Python code, improving code readability and organisation, generating scripts for data visualisation and plotting, refining SLURM job scripts for DelftBlue execution, converting algorithmic ideas into code, and assisting with CNF and DIMACS file generation and transformation.

Representative examples of implementation-related prompts included:

- "Why does this PWMC encoding generate too many clauses?"
- "Help debug this DIMACS formatting issue for Ganak."
- "Suggest a cleaner way to organise runtime experiment results into CSV files."

I reviewed and tested all AI-assisted code before using it. I validated the correctness of the implementation by testing on small graph instances for which expected reliability values could be computed manually or derived from the referenced literature. I inspected CNF encodings to ensure they correctly reflected the intended reliability formulation. When AI-generated code was incomplete or incorrect, I identified and fixed the issues myself.

## A.3. AI Usage During Writing

During the writing phase, I used generative AI to assist with improving grammar, spelling, and readability, restructuring paragraphs and sections, improving transitions and flow between explanations, generating draft outlines for thesis chapters, simplifying technical explanations, and formatting content in LaTeX.

Representative examples of writing-related prompts included:

- "Improve the flow between these two paragraphs without changing the meaning."
- "Rewrite this explanation in a more academic style."
- "Help structure the related work section."
- "Convert this explanation into LaTeX format."

I reviewed and revised all AI-generated text before including it in the thesis. I did not accept suggestions that changed my intended meaning or introduced claims I could not verify. I only included AI-generated suggestions after verifying their correctness and consistency with the rest of the thesis.

# B

# Constellation Visualisations

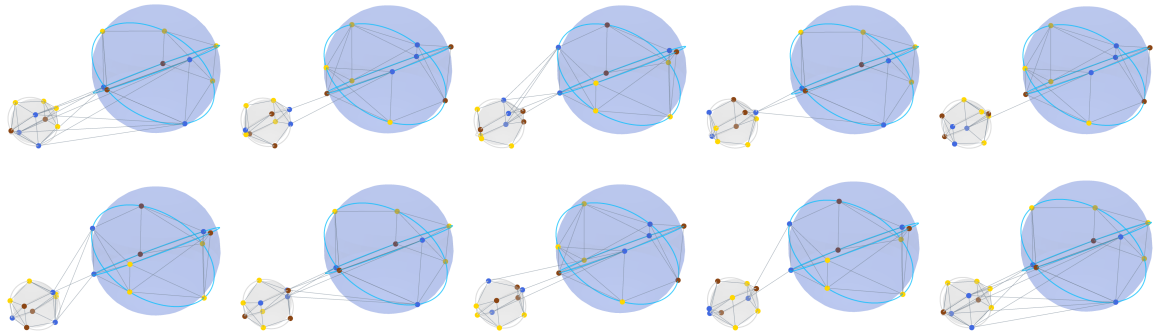

**Figure B.1:** Evolution of constellation C0 over the ten sampled timestamps. Brown satellites are ground-connected satellites, blue satellites are long-range satellites, and yellow satellites are short-range satellites.

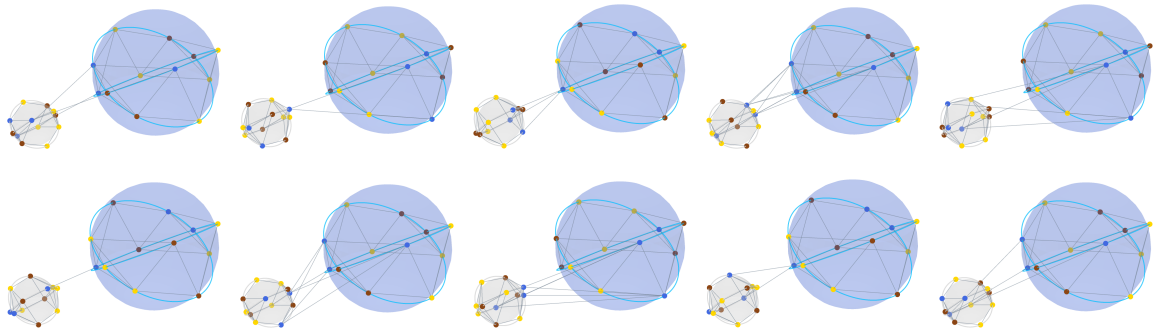

**Figure B.2:** Evolution of constellation C1 over the ten sampled timestamps. Brown satellites are ground-connected satellites, blue satellites are long-range satellites, and yellow satellites are short-range satellites.

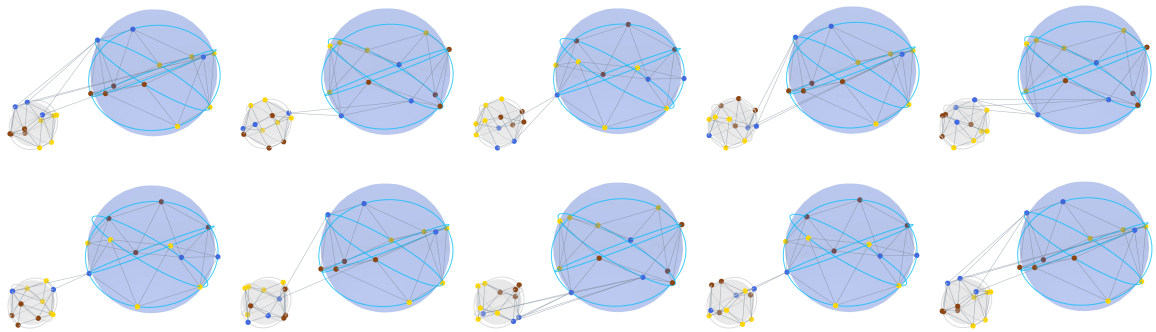

**Figure B.3:** Evolution of constellation C2 over the ten sampled timestamps. Brown satellites are ground-connected satellites, blue satellites are long-range satellites, and yellow satellites are short-range satellites.

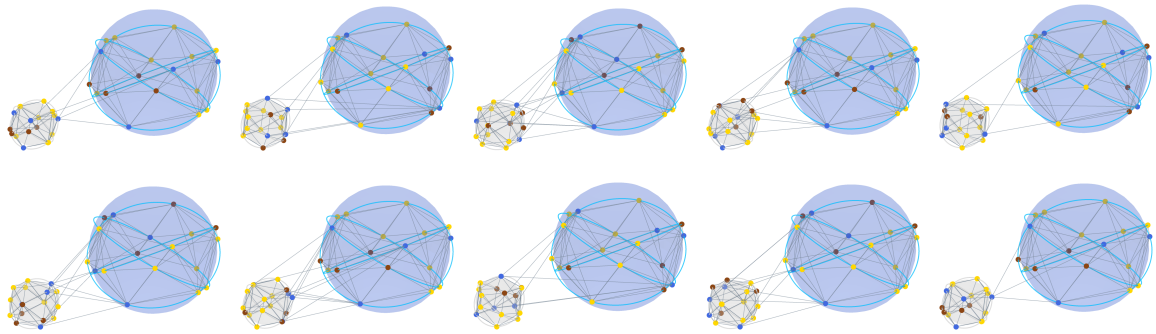

**Figure B.4:** Evolution of constellation C3 over the ten sampled timestamps. Brown satellites are ground-connected satellites, blue satellites are long-range satellites, and yellow satellites are short-range satellites.

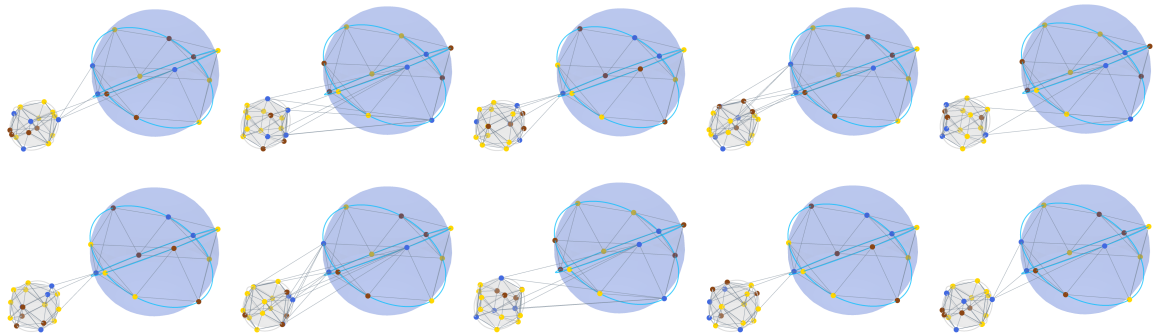

**Figure B.5:** Evolution of constellation C4 over the ten sampled timestamps. Brown satellites are ground-connected satellites, blue satellites are long-range satellites, and yellow satellites are short-range satellites.

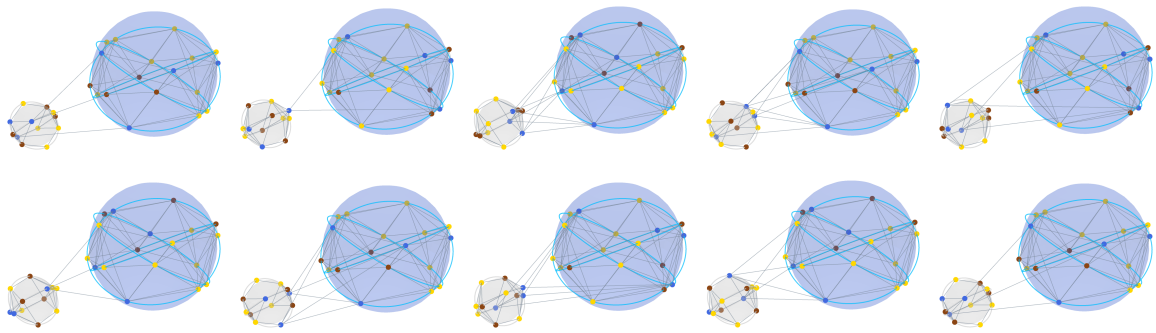

**Figure B.6:** Evolution of constellation C5 over the ten sampled timestamps. Brown satellites are ground-connected satellites, blue satellites are long-range satellites, and yellow satellites are short-range satellites.

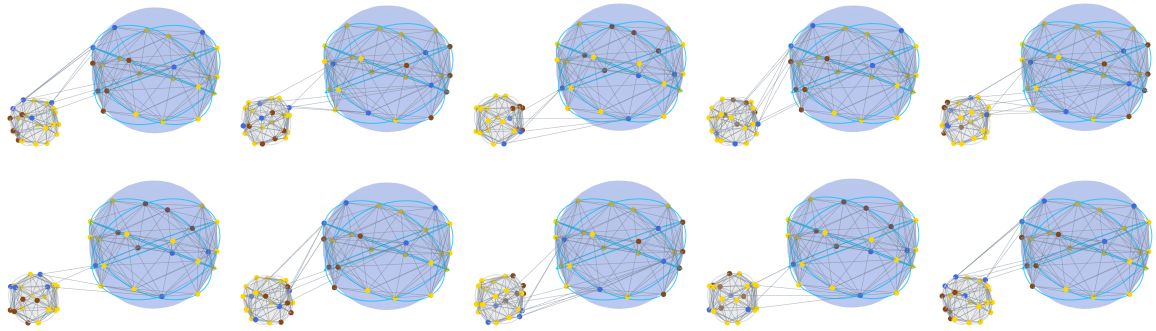

**Figure B.7:** Evolution of constellation C6 over the ten sampled timestamps. Brown satellites are ground-connected satellites, blue satellites are long-range satellites, and yellow satellites are short-range satellites.

# C

# Complete experimental results

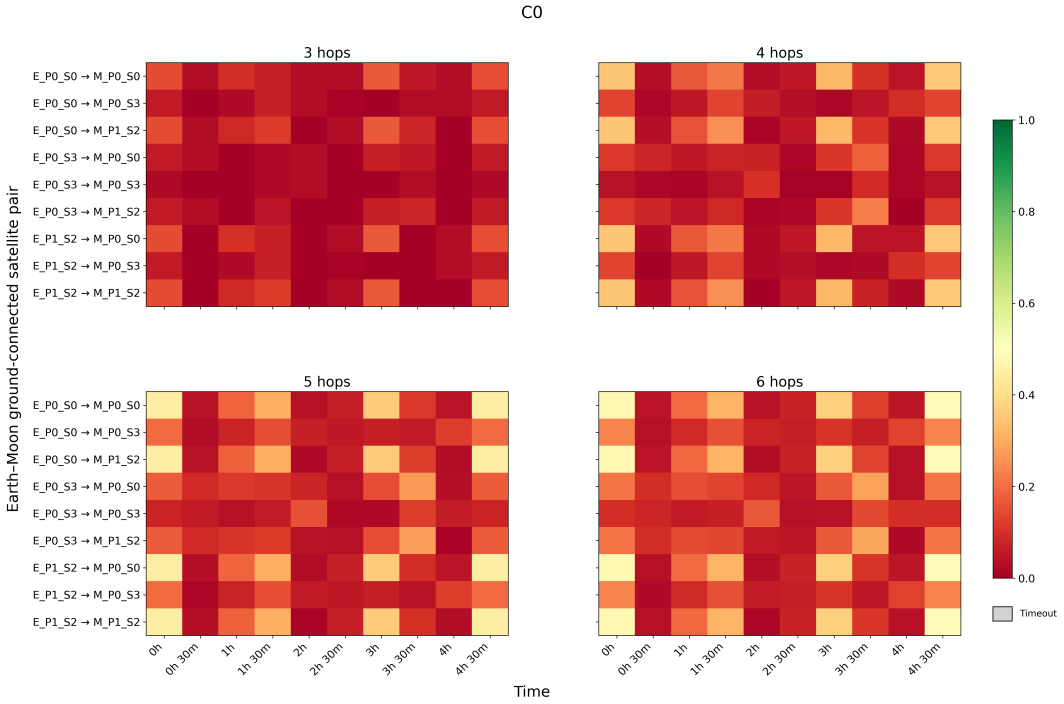


**Figure C.1:** Probability that a communication path of at most $k$ hops exists between each Earth–Moon ground-connected satellite pair over time for constellation C0. Results are computed using the reachability-based encoding, with path-based results used only when no reachability-based result is available.

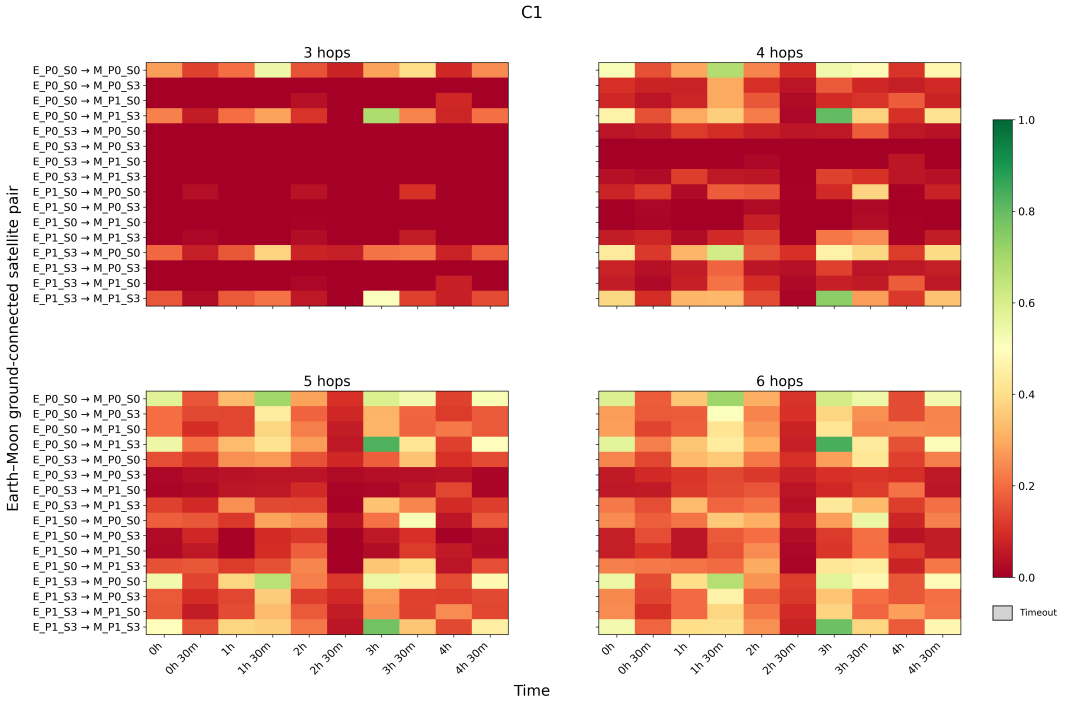


**Figure C.2:** Probability that a communication path of at most $k$ hops exists between each Earth–Moon ground-connected satellite pair over time for constellation C1. Results are computed using the reachability-based encoding, with path-based results used only when no reachability-based result is available.

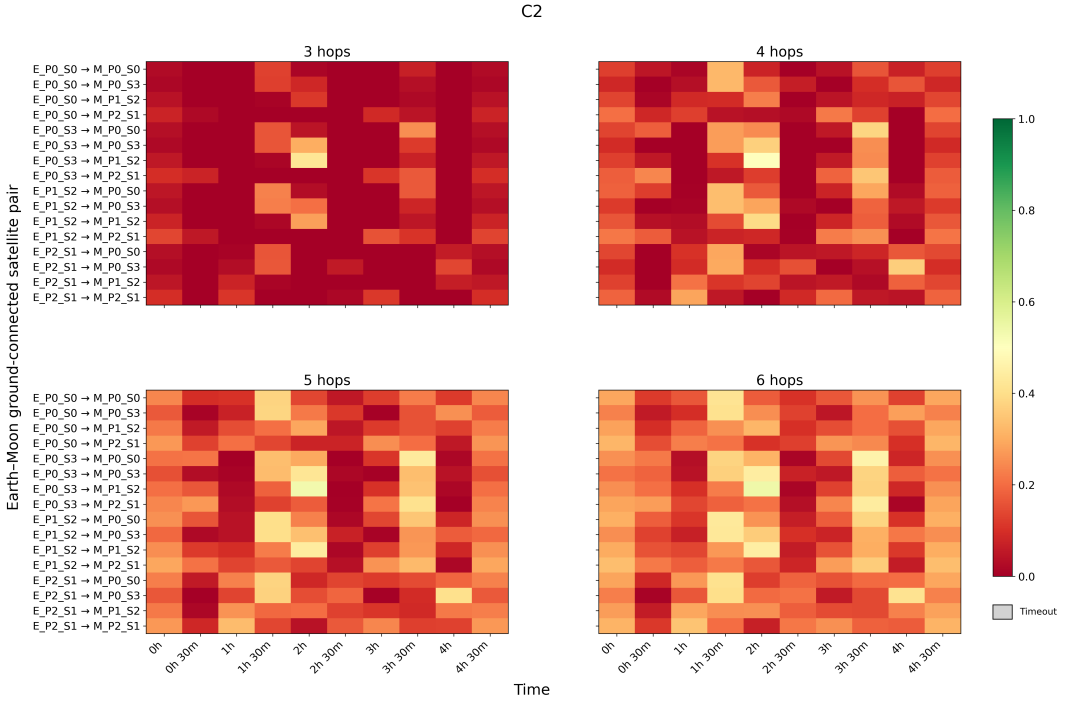


**Figure C.3:** Probability that a communication path of at most $k$ hops exists between each Earth–Moon ground-connected satellite pair over time for constellation C2. Results are computed using the reachability-based encoding, with path-based results used only when no reachability-based result is available.

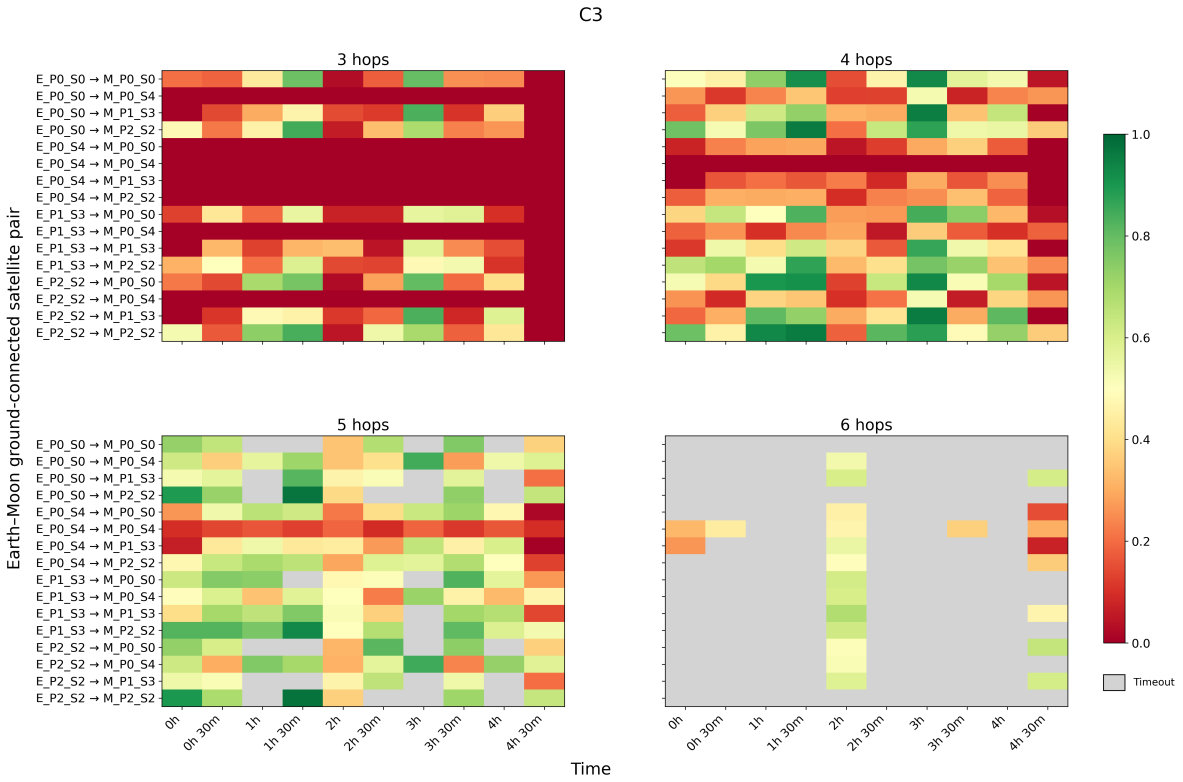


**Figure C.4:** Probability that a communication path of at most $k$ hops exists between each Earth–Moon ground-connected satellite pair over time for constellation C3. Results are computed using the reachability-based encoding, with path-based results used only when no reachability-based result is available.

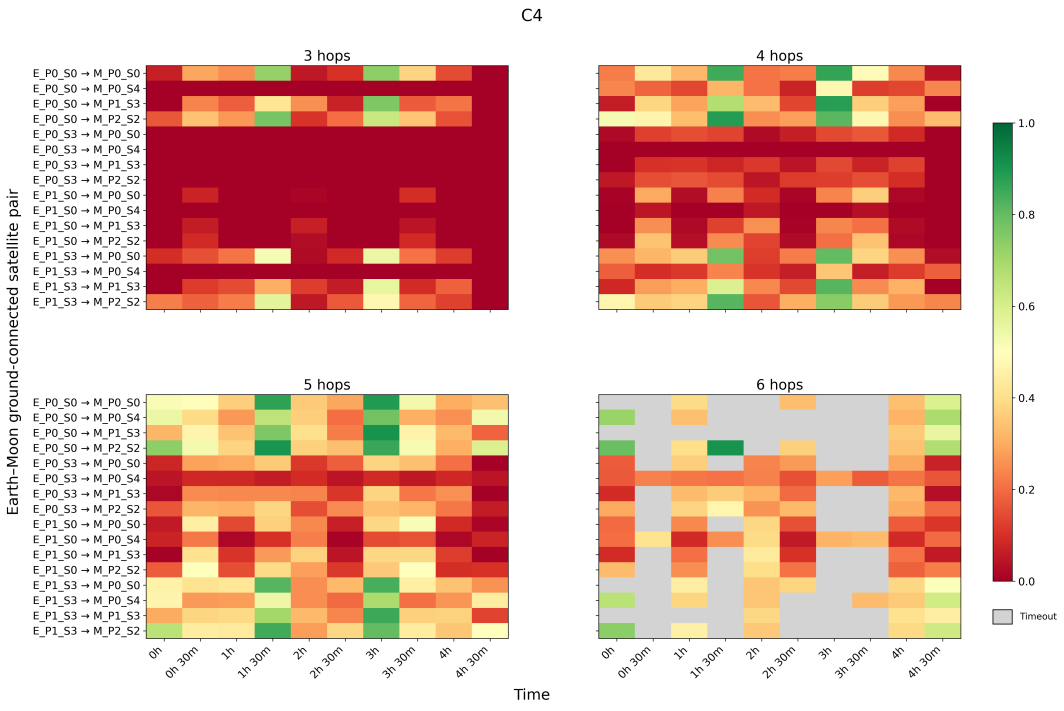


**Figure C.5:** Probability that a communication path of at most $k$ hops exists between each Earth–Moon ground-connected satellite pair over time for constellation C4. Results are computed using the reachability-based encoding, with path-based results used only when no reachability-based result is available.

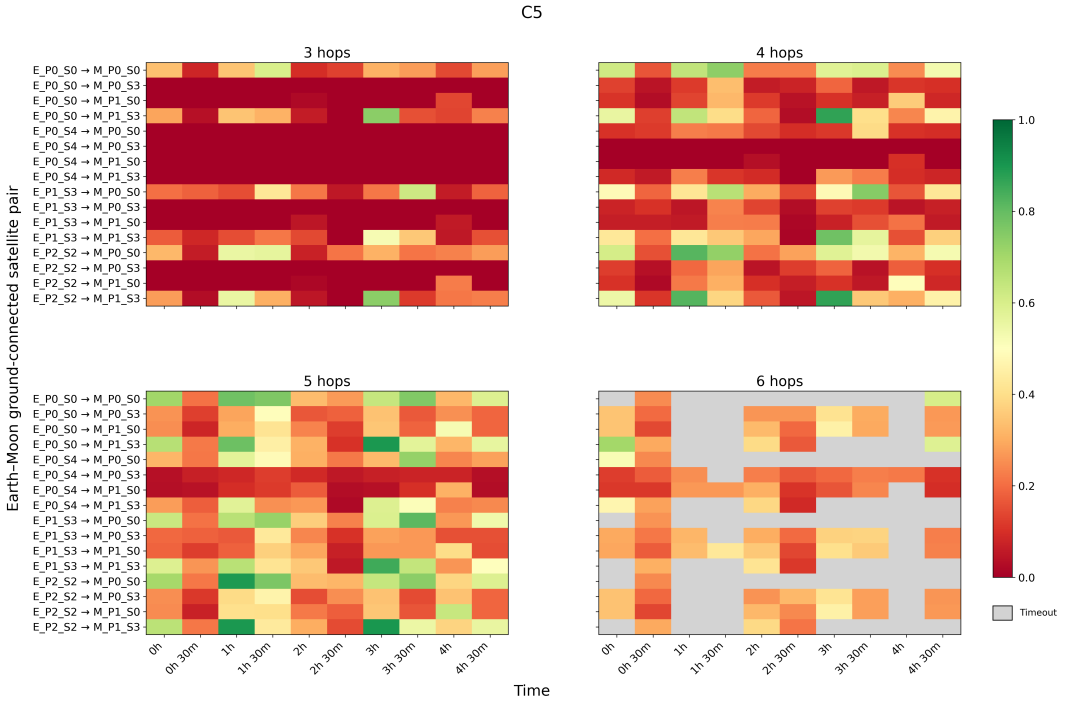


**Figure C.6:** Probability that a communication path of at most $k$ hops exists between each Earth–Moon ground-connected satellite pair over time for constellation C5. Results are computed using the reachability-based encoding, with path-based results used only when no reachability-based result is available.

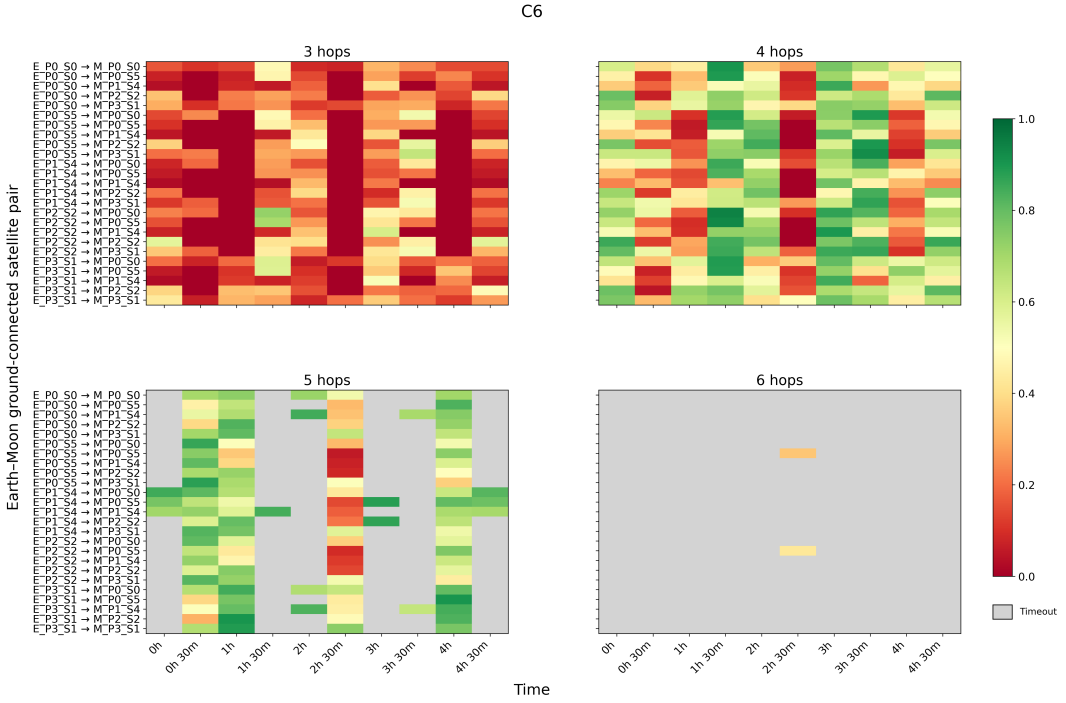


**Figure C.7:** Probability that a communication path of at most $k$ hops exists between each Earth–Moon ground-connected satellite pair over time for constellation C6. Results are computed using the reachability-based encoding, with path-based results used only when no reachability-based result is available.

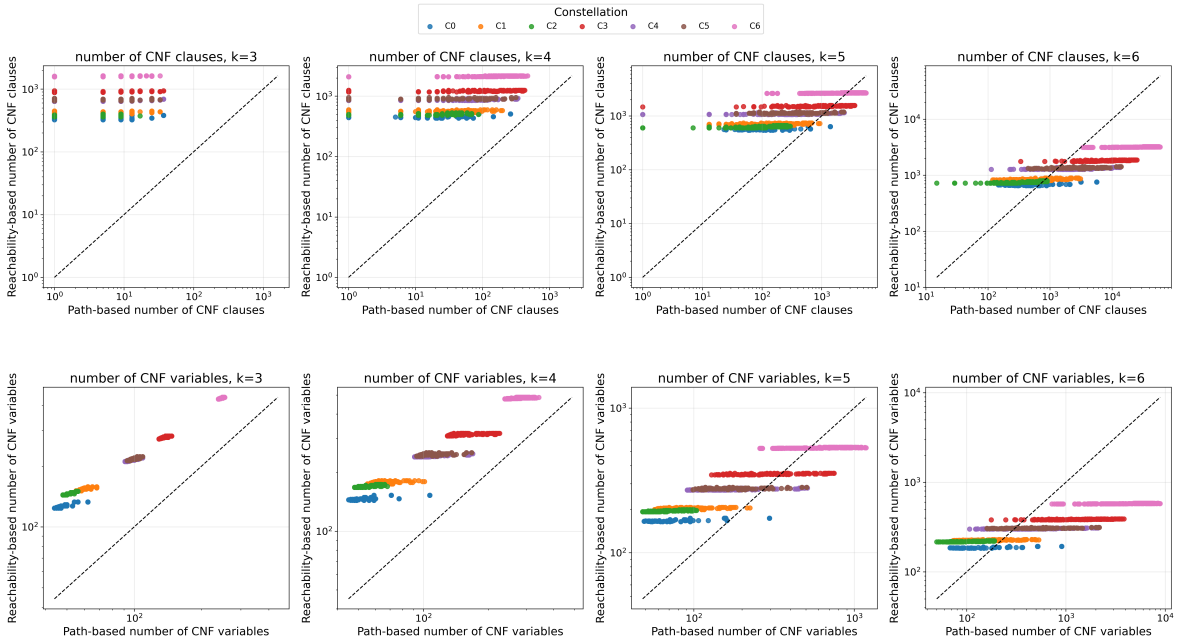


**Figure C.8:** Comparison of GANAK solving times for the path-based and reachability-based encodings on a logarithmic scale for hop limits $k = 3, 4, 5, 6$. Each point represents a ground-connected satellite pair at a given timestamp. Only instances solved by both encodings are shown.

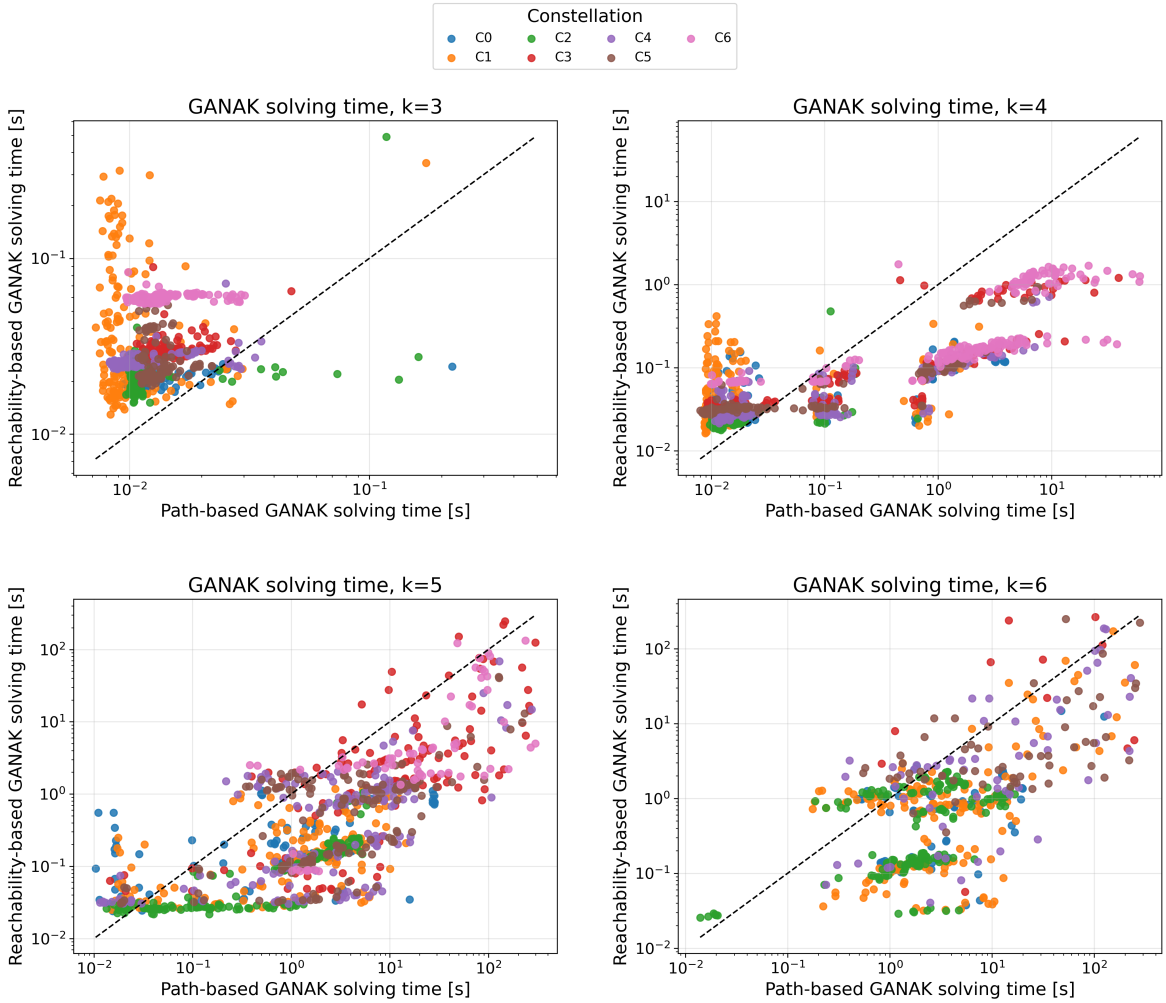


**Figure C.9:** Comparison of CNF model size for the path-based and reachability-based encodings on a logarithmic scale for hop limits $k = 3, 4, 5, 6$. Each point represents a ground-connected satellite pair at a given timestamp.

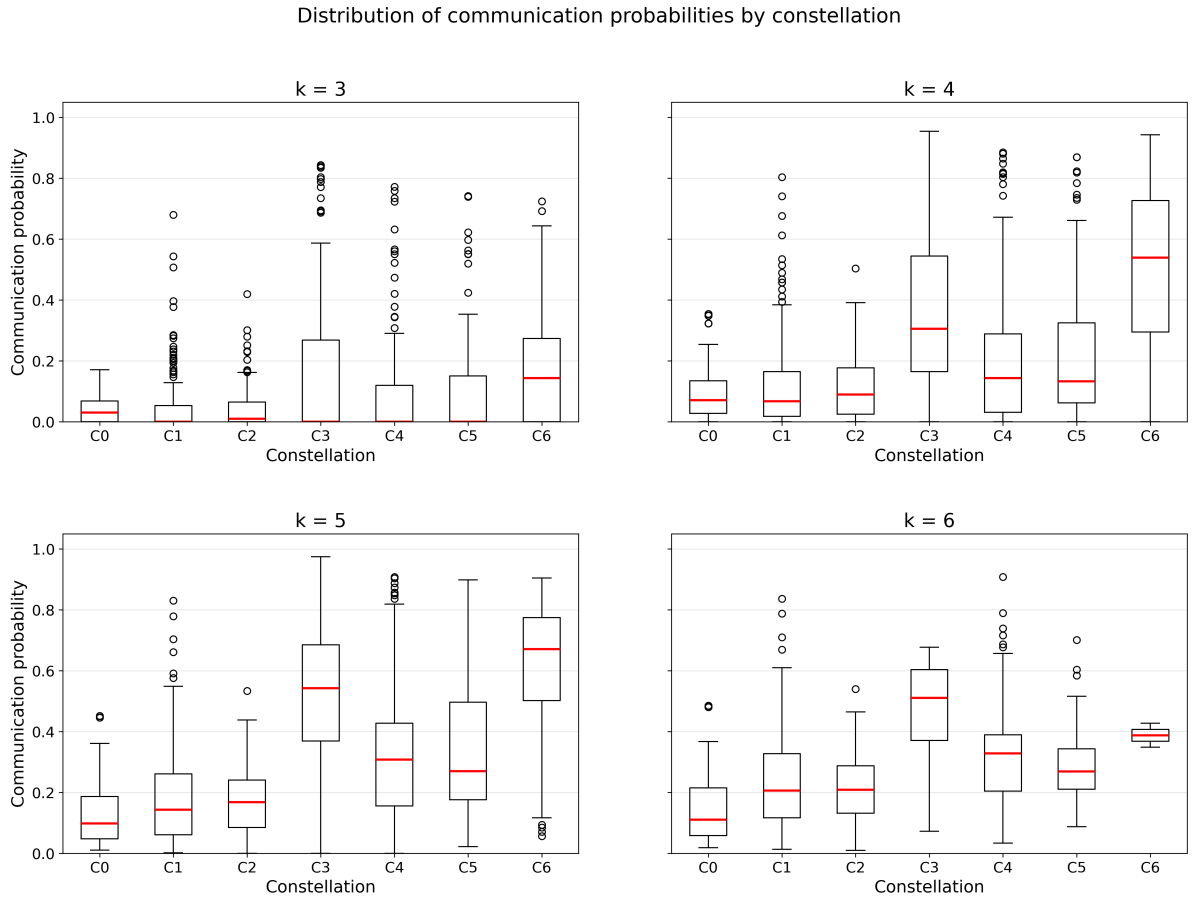


**Figure C.10:** Distribution of communication probabilities between Earth–Moon ground-connected satellite pairs for hop limits $k = 3, 4, 5, 6$. Each box summarizes all computed probabilities across evaluated timestamps and satellite pairs.